universität wien

MASTERARBEIT

„Chemische und biologische Charakterisierung von organometallischen Lapacholkomplexen und Untersuchungen von neuartigen naphthochinonbasierenden *O,S*-Chelaten“

Evelyn Balsano B.Sc.

angestrebter akademischer Grad

Master of Science (M.Sc.)

Wien, 2013

Studienkennzahl lt. Studienblatt:	A 066 862
Studienrichtung lt. Studienblatt:	Masterstudium Chemie
Betreuerin / Betreuer:	O. Univ.-Prof. Dr. Dr. Bernhard K. Keppler

universität wien

MASTER THESIS

„Chemical and biological characterization of organometallic lapachol complexes and investigations of novel naphthoquinone-based *O,S*-chelates“

Evelyn Balsano B.Sc.

Submitted in part fulfillment of the requirements for the degree

Master of Science (M.Sc.)

Vienna, 2013

Supervisor

O. Univ.-Prof. Dr. Dr. Bernhard K. Keppler

Auch eine Reise von tausend Meilen

beginnt mit dem ersten Schritt…

ACKNOWLEDGEMENTS

I would like to express my special thanks of gratitude

O. Univ.-Prof. Dr. Dr. Bernhard Keppler for the opportunity to work in his group on such an interesting topic.

My supervisor DI Dr. Wolfgang Kandioller for the unique, extraordinary and motivating support during my master thesis, for giving me the freedom of working independently and at the same time always being there whenever I needed him.

Mag. Dr. Michael Jakupec for giving me the possibility of performing the biological tests in his group and for the kind welcome.

The NMR service team (Dr. Sergey Abramkin, Dipl.-Chem. Paul-Steffen Kuhn, Mag. Verena Pichler, Mag. Michael Primik, DI Melanie Schmidlehner, and Ao. Univ.-Prof. Dr. Markus Galanski) for the NMR measurements.

Ao. Univ.-Prof. Dr. Arion and Ing. Alexander Roller for X-ray data collection and structure refinement.

Mag. Anatolie Dobrov and Mag. Aliona Luganschi for the mass spectra measurements.

Mag. Samuel M. Meier for the help and support concerning the ESI-MS measurements.

My laboratory colleagues Masha, Andrea, Stephan, Britta, Meli and Filip for the nice work atmosphere and for making Lab6 so extraordinary!

All members of the working group especially my friend Masha for the interesting, fruitful and motivating conversations and the countless funny, crazy and inspiring moments and adventures spent together besides university; Stephan for the good collaboration, scientific exchange, but also for the funny and open off-topic talks; Felix and Sepp for always being willing to help, and last but not least the cheerful and unforgettable time after work!

The whole biological group for welcoming me with open arms and letting me feel so indescribably well, for answering all my biological questions and for awakening my deep interest in working in the cell culture and making the work so attractive. Special thanks to Simone for the amazing support!

My Darling for being there in good times and being understanding and supportive in stressful times.

My parents and my sister Karin who have always believed in me and supported me with strengthening encouragement and never-ending love during my whole life. There are no words to express how deeply thankful I am for all you are doing for me to make all this possible!

For financial support: 

Johanna Mahlke geb. Obermann Foundation

ABSTRACT

Platinum-based chemotherapeutics have attracted great interest since the discovery of cisplatin by Barnett Rosenberg in the 1960ies. Clinically applied metallodrugs are cisplatin, carboplatin and oxaliplatin, which, however, display a broad spectrum of side effects, like nephrotoxicity, nausea, vomit, nerve damage, *etc*. Furthermore, tumor cells can develop resistance mechanisms, so that the patient stops to respond to the treatment.

Complexes that bear a ruthenium metal center are an auspicious alternative to the common platinum compounds. Ruthenium provides a series of advantages over platinum complexes: Ruthenium can mimic iron and can therefore bind to the transport protein transferrin. Tumor cells have a greater requirement for iron and hence possess a higher amount of transferrin receptors, because of their faster cell replication compared to healthy cells. Consequentially, a selective transport of ruthenium-based compounds to the cancer cell is possible.

Specific properties of the compounds can be fine-tuned with the accurate choice of the coordinated ligands influencing the biophysical properties, like water solubility and lipophilicity, but also the reactivity, and interaction with biomolecules.

Naphthoquinones are secondary plant metabolites, which display a broad spectrum of pharmacological characteristics (*e.g.* anticancer, antimicrobial, antiparasitic, and antiviral). The ligand system is able to generate intracellular reactive oxygen species (ROS) and by coordination to a metal center novel compounds with potential anticancer activity can be developed.

The aim of the master thesis was the synthesis of ruthenium-, osmium- and rhodium complexes with naphthoquinone derivatives as chelating ligands. The obtained organometallic compounds were characterized *via* 1D und 2D NMR spectroscopy, melting point, elemental analysis, and in two cases with X-ray diffraction analysis. Stability measurements with UV/Vis and ESI-MS were performed, and further interaction behavior and binding preferences of the compounds with amino acids and proteins *via* ESI-MS were investigated. The cytotoxic activity was determined by means of colorimetric MTT assay in different human cancer cell lines and the influence on the cell cycle, and the ability of reactive oxygen species generation was analyzed.

ZUSAMMENFASSUNG

Seit der Entdeckung von Cisplatin durch Barnett Rosenberg in den 1960er Jahren sind platinhaltige Zytostatika in der Chemotherapie von großer Bedeutung geworden. Cisplatin, Carboplatin und Oxaliplatin werden weltweit für die Behandlung von Krebs eingesetzt. Ein großer Nachteil dieser Verbindungen sind die vielseitigen Nebenwirkungen, wie Nephrotoxizität, Übelkeit, Erbrechen, Nervenschäden, *etc*. Zudem können Zellen Resistenzmechanismen bilden, sodass der Patient nicht mehr auf die Therapie anspricht.

Eine vielversprechende Alternative zu den gängigen Platinverbindungen sind Komplexe mit Ruthenium als Zentralatom, welches eine Reihe von Vorteilen besitzt: Durch die Ähnlichkeit zu Eisen wird es vom Transportprotein Transferrin aufgenommen und in die Zelle transportiert. Tumorzellen benötigen aufgrund ihrer höheren Zellteilungsrate mehr Eisen als gesunde Zellen. Sie besitzen deshalb eine größere Anzahl an Transferrinrezeptoren und es kann somit ein selektiver Transport von Rutheniumverbindungen in die Krebszelle erfolgen.

Durch die geeignete Wahl der Liganden können Substanzen mit spezifischen Eigenschaften konstruiert werden, wobei ein Einfluss in Hinsicht biophysikalischer Eigenschaften, wie Wasserlöslichkeit und Lipophilie, aber auch die Reaktivität, bzw. Wechselwirkung mit Biomolekülen erfolgt.

Naphthochinone sind natürlich vorkommende sekundäre Pflanzenmetabolite und besitzen ein breites Spektrum an pharmakologischen Eigenschaften (z. B.: tumorhemmend, antimikrobakteriell, antiparasitär und antiviral). Dieses Ligandensystem ist auch in der Lage intrazellulär reaktive Sauerstoffspezies (ROS) zu generieren und durch die Koordination an Metalle können neuartige Verbindungen mit potentieller Antitumoraktivität hergestellt werden.

Ziel der Masterarbeit ist die Synthese von Ruthenium-, Osmium- und Rhodiumkomplexen mit Naphtochinonderivaten als Chelatligand. Die organometallischen Verbindungen werden mit 1D und 2D NMR Spektroskopie, Schmelzpunktmessung, Elementaranalyse und in zwei Fällen mit Röntgenstrukturanalyse charakterisiert. Stabilitätsmessungen mit UV/Vis und ESI-MS werden durchgeführt, und ebenfalls die Wechselwirkung mit Aminosäuren und Proteinen mittels ESI-MS ermittelt. Die zytotoxische Aktivität wird mittels kolorimetrischem MTT Assay in verschiedenen humanen Krebszelllinien untersucht und

weiters der Einfluss auf den Zellzyklus, bzw. die Generierung reaktiver Sauerstoffspezies bestimmt.

TABLE OF CONTENTS

ABBREVIATIONS

1D/2D NMR ..... one- and/or two-dimensional NMR spectroscopy
A ..... adenine (nucleobase)
Å ..... Angstrom (10^{-10}m)
aa ..... amino acid
abs. ..... absolute, dry (solvent)
acac ..... acetyl acetonato ligand
cAMP ..... cyclic adenine monophosphate
°C ..... degree Centigrade
ben ..... benzene
bip ..... biphenyl
C ..... cytosine (nucleobase)
Cdc ..... cell division cycle
$CDCl_3$ ..... deuterated chloroform
CDK ..... cyclin-dependent kinase
Cp* ..... 1,2,3,4,5-pentamethylcyclopentadienyl ligand
CREB ..... cAMP response element-binding protein
cyc ..... cyclin
cys ..... cysteine
p-cym ..... *p*-cymene
δ ..... chemical shift (NMR)
d ..... doublet (NMR)
DCFH-DA ..... 2',7'-dichlorofluorescin diacetate
DCM ..... dichloromethane
DHA ..... dihydroanthracene
DNA (CT-DNA) ..... desoxyribonucleic acid (calf thymus DNA)
DMSO-d_6 ..... deuterated dimethyl sulfoxide
dppz ..... dipyrido[3,2-a:2',3'-c]phenazine
e.g. ..... *exempli gratia* (for example)
EGFR ..... epidermal growth factor receptor
en ..... ethylenediamine
ERK ..... extracellular signal-regulated kinases
eq ..... equivalent

ESI-MS ..... electronspray ionization - mass spectrometry

et al. ..... *et alii* (and others)

EtG 9-ethylguanine

EtOH ..... ethanol

FACS ..... fluorescence activated cell sorting

Fhit ..... fragile histidine triad protein(Bis(5'-adenosyl)-triphosphatase)

G ..... guanine (nucleobase)

GC-MS ..... gas chromatography - mass spectrometry

Gly ..... glycine

dGMP ..... deoxyguanosine monophosphate (deoxyguanylate)

h ..... hour

HeLa ..... human epithelial carcinoma cell line

hept ..... heptet (NMR)

His ..... histidine

HMG ..... high mobility group

HPLC ..... high performance liquid chromatography

IT ..... ion trap

HT29 ..... human colon adenocarcinoma grade II cell line

(M)Hz ..... (mega)hertz (s^{-1})

MTT ..... 3-(4,5-dimethylthiazol-2-yl)-2,5-diphenyltetrazolium bromide

NMM ..... N-methylmorpholine

NXO2 ..... human lung cancer cell line

IC_{50} ..... drug concentration that causes 50% cell growth inhibition

INF-ɣ ..... interferon-gamma

J ..... coupling constant (NMR)

(m/µ/n)M ..... (milli/micro/nano)molar (mol / L; mmol / L; µmol / L; nmol / L)

m ..... multiplet (NMR)

MCa ..... mammary carcinoma

Met ..... methionine

min ..... minute

MeOH ..... methanol

myc ..... v-myc myelocytomatosis viral oncogene homolog (avian)

NMR ..... nuclear magnetic resonance spectroscopy

Pank-1 ..... human pancreatic carcinoma, epithelial-like cell line

PBS ..... phosphate buffered saline
i-PrOH ..... isopropanol
pH..... pondus Hydrogenii (power of hydrogen)
phen ..... phenanthroline
phi ..... phenanthrene quinone diimine
phzi..... benzo[a]phenazine-5,6-quinone diimine
Pim-1 ..... proto-oncogene serine/threonine-protein kinase
pKa..... -log K_a (acid dissociation constant)
pp ..... polypyridyl
ppm ..... parts per million
PTA 1,3,5-triaza-7-phosphaadamantane
PTP ..... protein tyrosine phosphatase
RAPTA ..... ruthenium (II) arene PTA
Ras..... rat sarcoma
Rb..... retinoblastoma protein
RNA, mRNA, miR..... ribonucleic acid, messenger RNA, microRNA
ROS ..... reactive oxygen species
r.t. ..... room temperature
s ..... singlet (NMR)
SIM..... selective ion monitoring
SK-N-SH ..... human neuroblastoma cell line
T ..... thymine (nucleobase)
t ..... triplet (NMR)
Tcl ..... T-cell leukemia/lymphoma
td ..... triple doublet
THA..... tetrahydroanthracene
TOF ..... time-of-flight
TPA 12-O-tetradecanoylphorbol-13-acetate
Ub..... ubiquitin
UV/Vis ..... ultraviolet/visible
Walker 256 ..... rat breast carcinoma cell line
WHO ..... World Health Organization

1 INTRODUCTION

1.1 STATISTICS AND FACTS ABOUT CANCER

Cancer is a leading cause of death worldwide, accounting for 7.6 million deaths (around 13% of all deaths) in 2008[1] and the total number of cases globally is increasing. Cancer causes more deaths than AIDS, tuberculosis, and malaria combined.[2] According to World Health Organization (WHO) projections in 2007, cancer will have replaced ischemic heart disease as the overall leading cause of death worldwide in 2030 (see Figure 1).

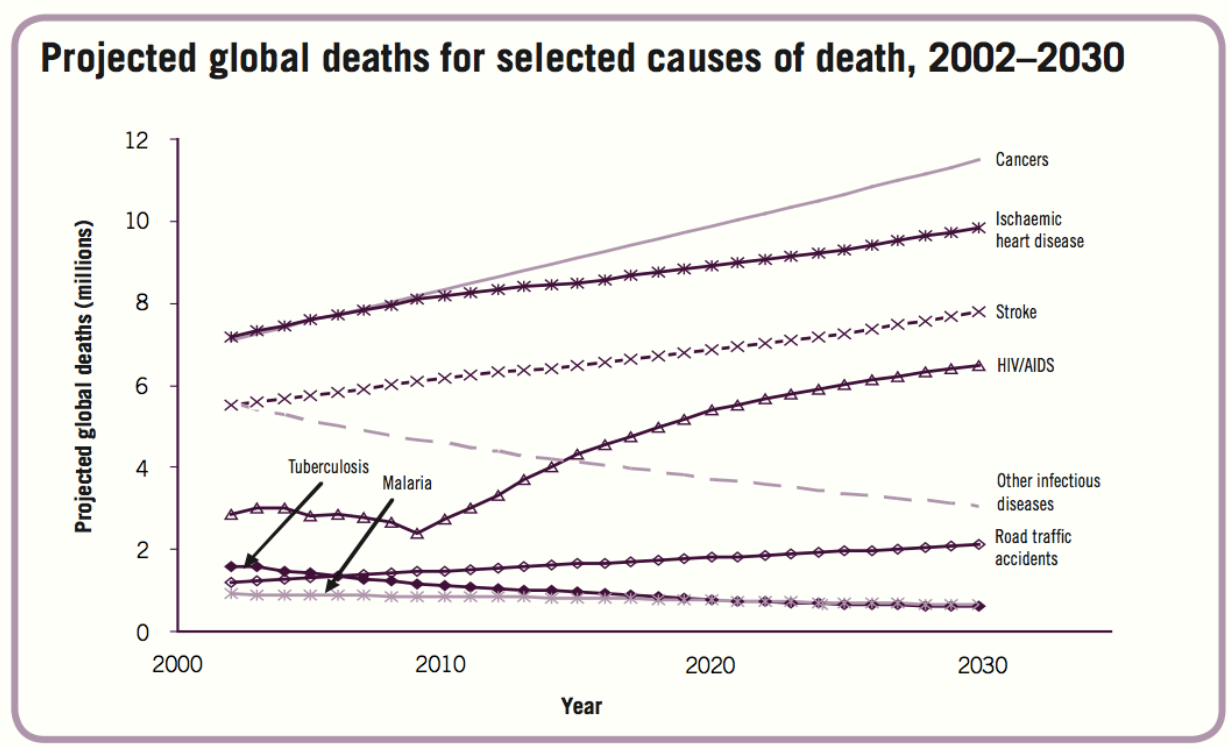

Figure 1: Projected deaths for selected causes in 2030[3]

One person in three is likely to develop cancer during lifetime. Every tissue and every organ of the human body can in principal be impacted by this disease. However, there is a large variation in the frequency depending on the age, sex, ethnicity, geographical region, alimentary habits, and similar factors. Studies of population environments reveal carcinogenic agents, *e.g.* food (stomach cancer, colon cancer), smoking (lung cancer),

[1] http://globocan.iarc.fr/factsheets/populations/factsheet.asp?uno=900 (retrieved nov 12, 2012).

[2] http://www.cancer.org/acs/groups/content/@epidemiologysurveilance/documents/document/acspc-027766.pdf (retrieved nov 16, 2012).

[3] http://www.who.int/whosis/whostat2007_10highlights.pdf (retrieved nov 16, 2012).

excessive exposure to sunlight (skin cancer), or exposure to radiation (leukemia).[4] The mortality rate varies for different types of cancer. Lung cancers (including trachea and bronchus cancer) are the most common cause of death from cancer among men, followed by stomach, colon and rectum, esophagus, and prostate cancer. For women, the most common cancer at global level is breast cancer, followed by cancers of the trachea, bronchus and lung, and stomach cancer.[5]

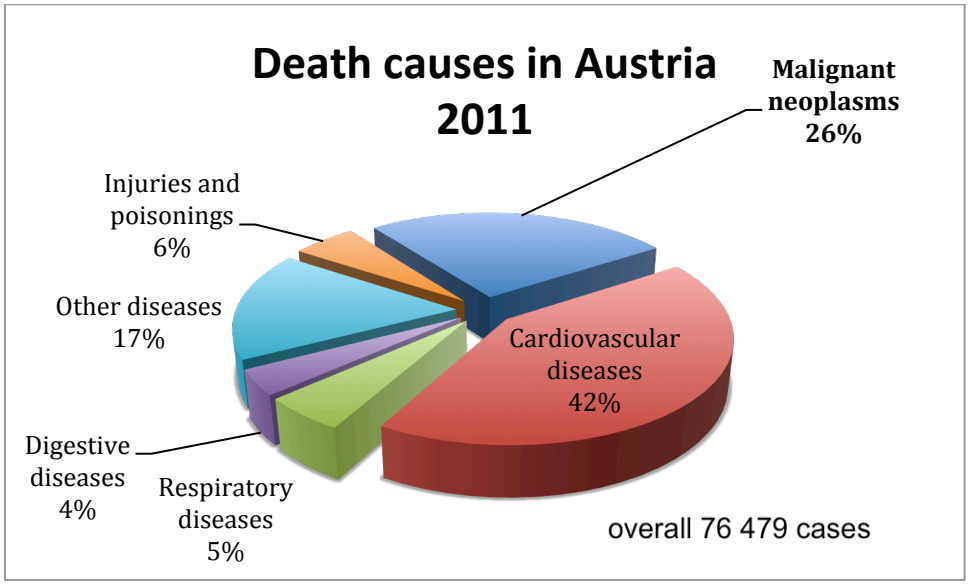

Figure 2: Percental death causes in Austria in 2011. Malignant neoplasms causing a quarter of the number of death cases[6]

In Austria annually, 37 000 to 38 000 people get cancer, among them slightly more men than women are affected. Colon, lung, breast, and prostate cancer are the most common cancer diseases. For both sexes, malignant neoplasms are the second most common cause of death after cardiovascular diseases. In Austria in 2011, 76 479 people died, 52% women and 48% men. Diseases that are more frequent in higher age become evermore the leading death causes, due to the aging of the population. Figure 2 shows the death causes in Austria in 2011. Malignant neoplasms caused death for 10 576 men and 9 416 women, being responsible for a quarter of the annual number of deaths. The leading cancer causes of death for men are lung, prostate, colon, and pancreatic cancer; for women breast, followed by lung cancer, cancer of the lymphatic and hematopoietic tissue, and pancreatic cancer. Figure 3 shows the incidence and

[4] Paradee A. B., Stein G. S.; The Biology and Treatment of Cancer, **2009**.
[5] http://www.who.int/healthinfo/global_burden_disease/GBD_report_2004update_part2.pdf (retrieved nov 12, 2012).
[6] based on the data from Statistik Austria http://www.statistik.at/web_de/statistiken/bevoelkerung/sterbefaelle/index.html (retrieved nov, 9 2012).

mortality of different cancer types for men and women in Austria in 2009. Tendentially, both - the risk for a new incident and the mortality risk in Austria - are decreasing, due to earlier diagnostics and new therapy methods. A particularly strong decrease is observable for the incidence of stomach cancer (according to the data of Statistik Austria between 1994 and 2010). Epidemiologically, this can be explained due to changed nutrition, and an improved storage and cooling technology.

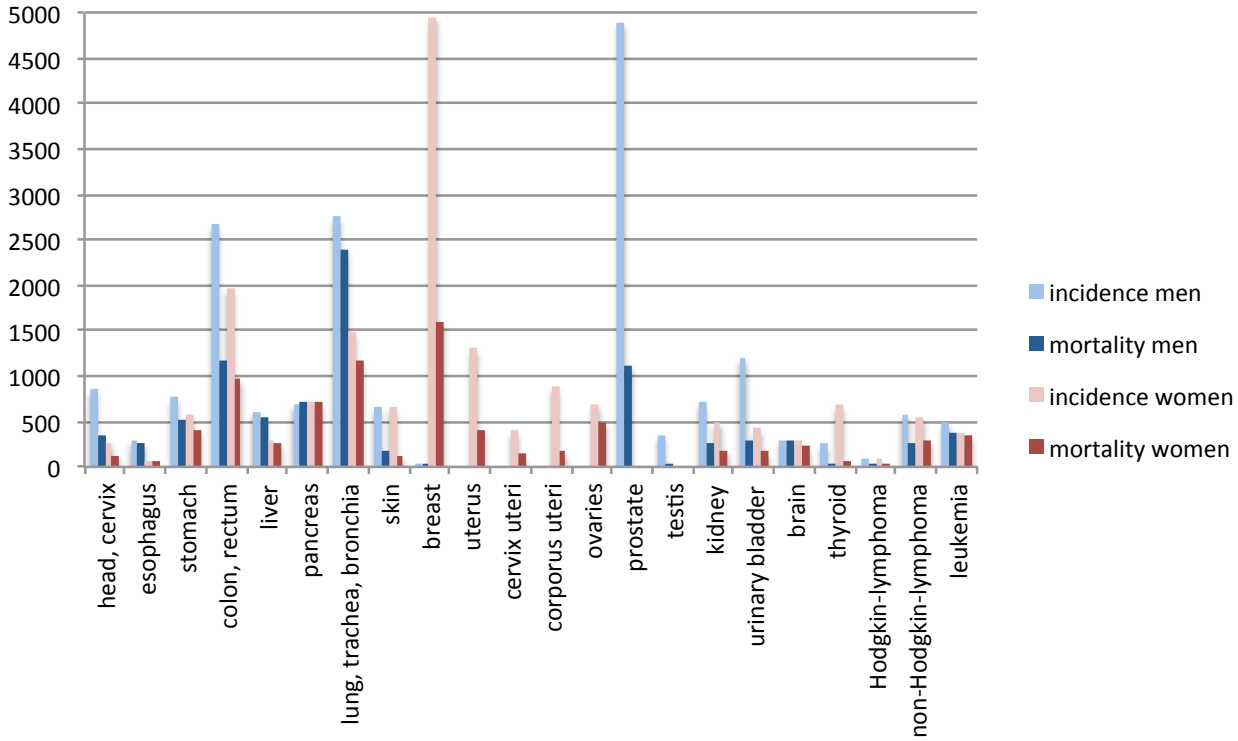

Figure 3: Cancer incidence and mortality among men and women in Austria in 2009[7]

[7] http://www.statistik.at/web_de/statistiken/gesundheit/krebserkrankungen/krebsinzidenz_im_ueberblick/index.html.

1.2 BIOLOGY OF CANCER

Cancer is not a single disease, but a group of diseases characterized by uncontrolled growth and spread of abnormal (mutated) cells. Metastasis causes 90% of cancer deaths. There are about 200 varieties of cancer, which can be classified into 3 main types: carcinomas (90%) which are solid tumors of epithelial cells of inner and outer surfaces, sarcomas which are derived from muscle or bone, and leukemias and lymphomas which are not solid cancers of white blood cells.[4] Cancer is caused by both external factors (tobacco, chemicals, radiation, and infectious organisms) and internal factors (inherited mutations, hormones, immune conditions, and mutations that occur from metabolism). These causal factors may act together or in sequence to initiate or promote carcinogenesis. The development of most cancers requires multiple steps that occur over many years. Often, detection of cancer occurs ten or more years after exposure to external factors.[8]

1.3 CANCER DEVELOPMENT/CARCINOGENESIS

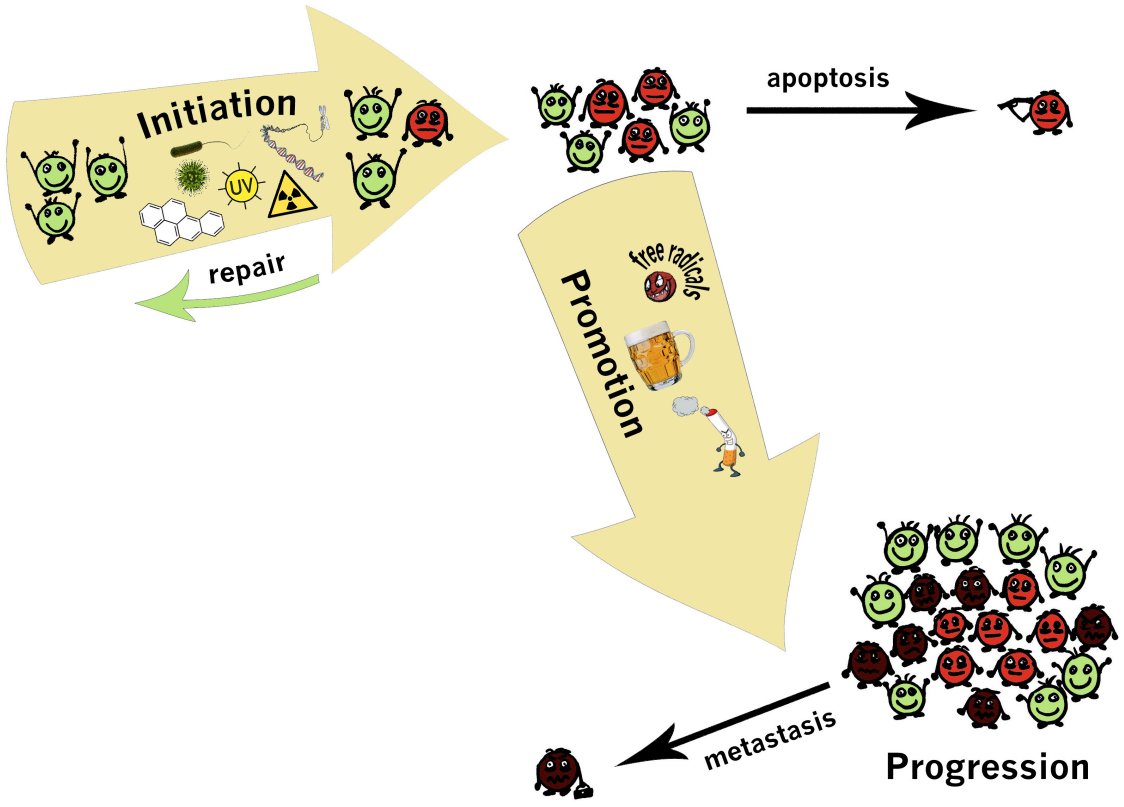

Figure 4: Three-step model of carcinogenesis

[8] http://www.scripps.edu/discover/cancer.htmlhttp://www.scripps.edu/discover/cancer.html (retrieved nov 19, 2012).

A classical three-step model of carcinogenesis (see Figure 4) describes the development of cancer. The individual steps are initiation, promotion and progression (malignant transformation). Initiators are mutagens and may, like alkylating agents, be themselves chemically reactive or they may be substances that are transformed into chemically reactive agents by metabolic processes. The active reagents may react with DNA, induce damage and cause mutation. The active mutagenic forms of polycyclic hydrocarbons are epoxide derivatives and the reactive products of aromatic amines are hydroxylamine derivatives. Initiation can occur from chemicals (*e.g.* hydrocarbons, nitrosamines, nickel powder, ingredients of tobacco), radiation sources (*e.g.* ionizing radiation, UV-light, radioactive radiation, X-rays), viruses (*e.g.* human papilloma virus, hepatitis B virus), and bacteria, or inherited predisposition. Mutations are errors in the DNA that alter the genetic information. When molecular mechanisms (checkpoints) sense the damage, cell growth is stopped, enzymes for repair are activated and recover is possible, or the cell undergoes the programmed cell death (apoptosis). Accumulated alterations, especially of protein-coding genes (details see below), may result in cancer.

The second step of the model is induced by tumor-promoters (*e.g.* phorbol ester TPA, hormones, asbestos, estrogenes, alcohol, smoke), which are non-reactive and not cancerogenous compounds itself, but enhance tumor formation by inhibition of apoptosis and stimulation of cell growth (proliferation). Promotion often entails the production of free radicals and the induction of “benign” lesions.

Some compounds have initiating and promoting activity and are called complete carcinogens, because tumor development can occur without the application of another compound.

When the last step, tumor progression (malignant transformation) occurs, the first lesions are changed into malignant cancers. Malignant cancer cells grow uncontrolled, break down the tissue surrounding them, invade their environment, and attract new blood vessels (angiogenesis). Spreading of tumor cells out of the primary tumor (metastasis) is possible.[9]

However, cancer development is more complex, and today, a multi-step model, which is not fully understood yet, is supposed. There are different theories about tumor emergence. According to a new model, the “feedback loop” model of carcinogenesis,

[9] Boyland, E., *Br J Ind Med*, **1985**, 42, 716-8.

not only mutations in the cell, but also the microenvironment are strongly involved in carcinogenesis.[10]

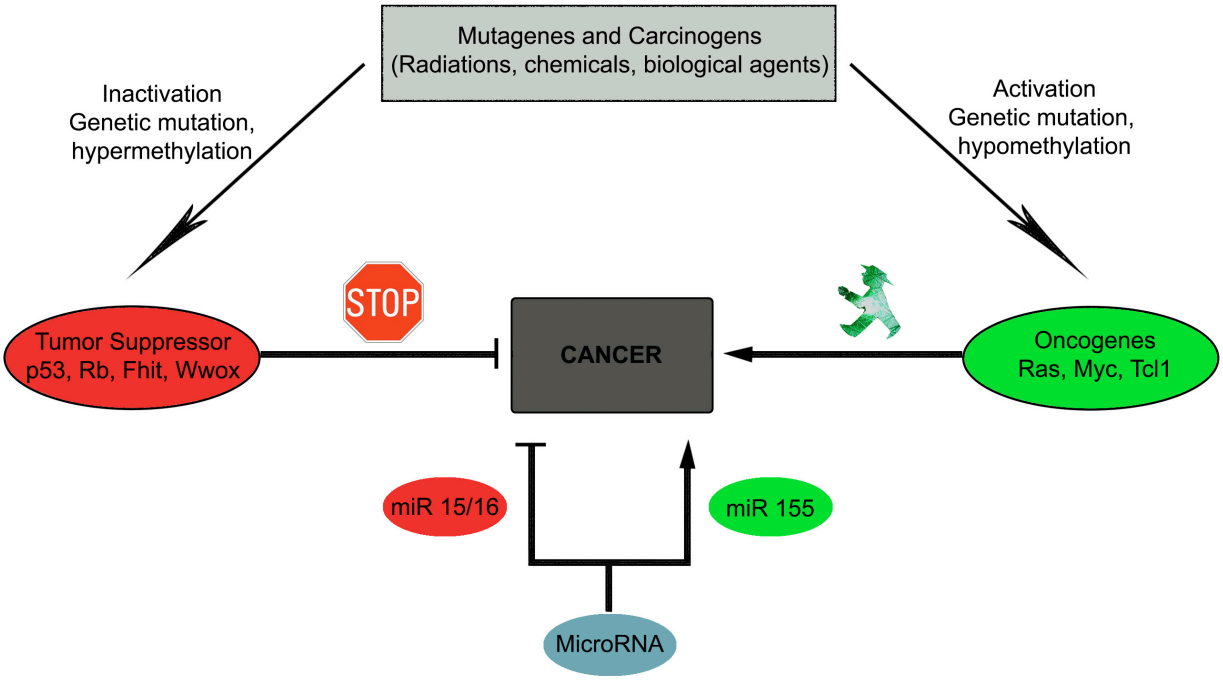

Figure 5: Schematic representation how genetics, epigenetics, and environmental factors (radiations, chemicals, and microorganisms) are related in causing cancer.[4]

Figure 5 shows the complex relationships among genetics, epigenetics and environmental factors in causing cancer. Alterations of protein-coding genes, like oncogenes, tumor suppressor genes, and stability genes, are often found in cancers. Oncogenes encode proteins that control cell proliferation, apoptosis, or both; they are activated in cancer, which makes them suitable targets for gene-specific cancer treatment. Tumor suppressor genes protect the cell to progress to cancer. When the gene is mutated it comes to a loss of this function. Tumor suppressor inactivation can occur in both sporadic and inherited cancer predisposition syndromes, secondly is not the case for oncogene activation. Another group are the stability genes, which act in repairing mechanisms, and keep genetic alterations to a minimum. If these genes are inactivated, mutations in other genes, such as oncogenes and tumor suppressor genes, take place. Recently, another group of noncoding-genes, mi-RNA, have been shown to be involved in the development of cancer.[4]

[10] Rückert, F.S., C.; Niedergethmann, M., *Communicative&Integrative Biology*, **2012**, 5, 506-07.

1.4 CELL CYCLE

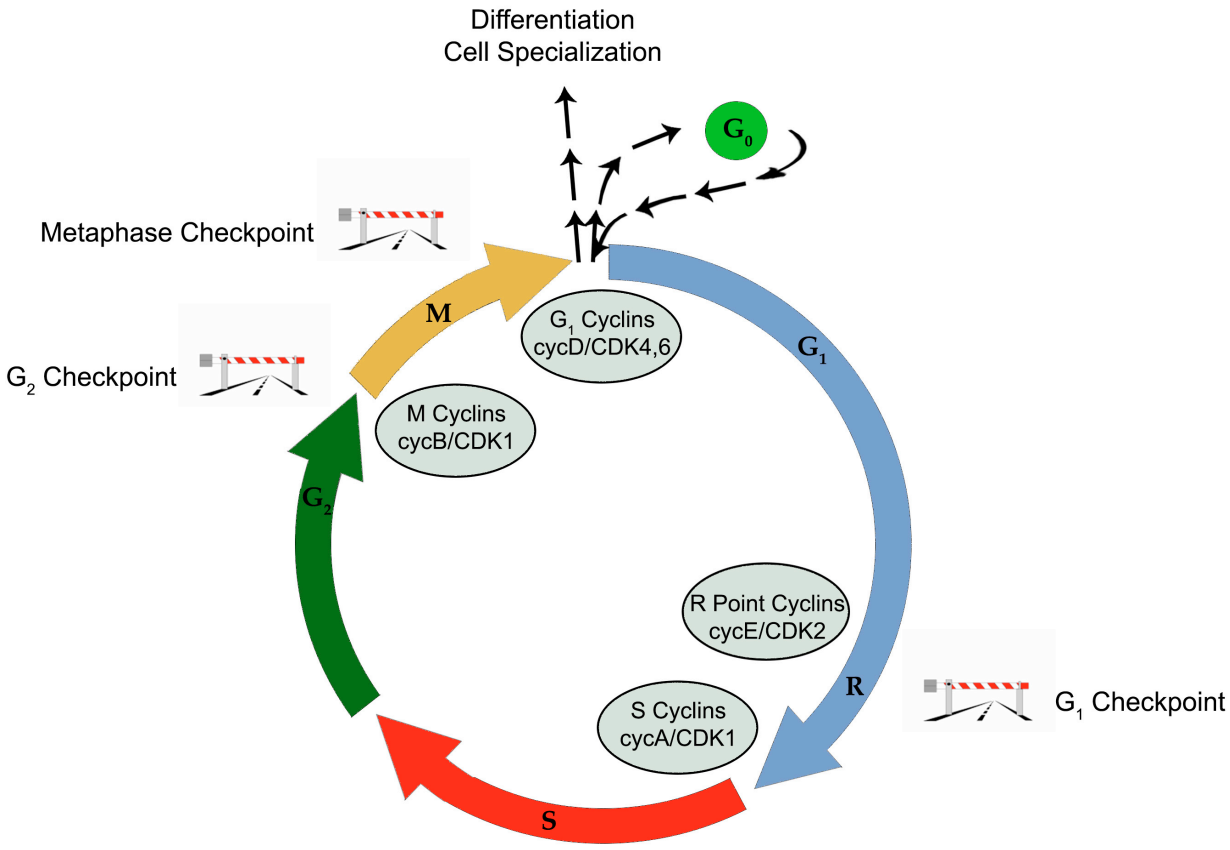

Figure 6: The stages of the cell cycle[4]

An important interest to cancer research is the cell cycle, which a cell undergoes in order to duplicate (Figure 6). It consists of four biochemically different phases, G_1, S, G_2 and M, followed by division. The cell is regulated by cyclins (cyc) and cyclin-dependent kinases (cdk) that regulate genes during each period. Their concentration increases and decreases at definite times in the cell cycle. In G_1 the molecular machinery for DNA is produced and activated. Cyclin D1 activates a cyclin-dependent kinase (cdk) that phosphorylates proteins that control progression through the cell cycle. It is overexpressed in many tumors (*e.g.* 50% of breast cancer). Synthesis of DNA occurs during the S Phase. Histones are synthesized to package newly replicated DNA into chromosomes. The short G_2 phase follows, which prepares the cell to enter mitosis (M phase). During M phase duplicated chromosomes are distributed equally prior the cell division. In the case of cancer, errors in the separation may take place, especially if the DNA is damaged. Mutations lead to disturbances of the cycle and so to cancer. Among the most frequently mutated proteins are the cyclins; the retinoblastoma protein, which

inactivates protein E2F-1 and thereby disrupts the copying of many genes into their mRNA; and the p53 protein, which activates the programmed cell death mechanism, which can eliminate cancer cells. As a consequence cells can multiply in an uncontrolled way.[4]

Understanding the cell cycle and investigating the specific effect of cancer drugs is nowadays an important parameter for drug design. Many drugs for example work only on cells that are actively reproducing (and not cells that are in the resting phase, G_0). Some compounds alter the expression and the activity of key proteins involved in the regulation of the cell cycle, which leads to apoptosis; some attack cells only in a particular phase, and can lead to a characteristic cell cycle arrest.

1.5 CANCER THERAPY

From 1992 to 2003, cancer death rates have declined due largely to a decrease in the use of tobacco, improved screening techniques, and advances in treatment. The most common approaches for cancer treatment include surgery, radiation therapy, chemotherapy, immunology, and hormone therapy.[4] The choice of treatment depends on the location and grade of the tumor, the stage of the disease, and the general state of the patient.

Surgery: Operative removal of the solid tumor or the entire organ is the oldest form for cancer treatment and is still the most effective in early stage of the disease and localized metastasis.

Radiation therapy: Radiation therapy uses high-energy radiation (ionizing radiation, photon, X-ray, ɣ-ray or charged particles) to control or kill malignant cells by damaging the DNA and therefore leading to cellular death. It can be used to cure (curative), to destroy any remaining cancer cells after surgery in order to prevent recurrence (adjuvant), and to control local disease or relief the symptoms (palliative). The radiation can be generated by a machine outside the body, or it can be delivered in form of radioisotopes, which may be implanted in the body near tumor cells, or administered into the bloodstream. Radiation therapy can also damage normal cells, leading to side effects, which are usually limited to the area of the patient's body that is under treatment. The main common side effects reported are fatigue and skin irritation. Late side effects are possible and include fibrosis, damage of the bowels, causing diarrhea and bleeding, memory loss, and infertility. Rarely a second cancer incident can be

caused.[11]

Chemotherapy:[12] Generally the expression chemotherapy refers to the use of drugs to treat any kind of disease. The two medicinal terms antineoplastic (anti-cancer) therapy and cytotoxic (cell-killing) therapy are used to describe cancer chemotherapy. Chemotherapy differs from surgery or radiation in that it is almost always used as a systemic treatment. This means the drugs travel throughout the body to reach cancer cells. Chemotherapy is used to treat many cancers. More than 100 chemotherapy drugs are used today. They vary widely in their chemical composition, their administration, their response on specific forms of cancer, and their side effects. According to their various properties chemotherapeutics are classified into the following groups.[13]

- Alkylating agents (*e.g.* mechlorethamine, streptozocin) directly damage DNA by covalent binding to nucleic bases, either by cross-linking of the two strands of DNA or DNA breakage, to prevent the cancer cell from reproducing. All alkylating agents are not phase-specific; that means they work in all phases of the cell cycle; they kill rapidly proliferating cells, but also non-proliferating cells. Alkylating agents are used to treat many different cancers, including leukemia, lymphoma, Hodgkin disease, multiple myeloma, sarcoma, as well as cancers of the lung, breast, prostate and ovary. Because these drugs damage DNA, they can cause long-term damage to the bone marrow. The platinum drugs (cisplatin, carboplatin, and oxaliplatin) are classified as alkylating-like agents, because they kill cells in a similar way.
- Antimetabolites (*e.g.* 5-fluorouracil, hydroxyurea, thioguanin) interfere with DNA and RNA growth by mimicking the normal building blocks of RNA and DNA. These agents damage cells during the S phase. They are commonly used to treat leukemia, cancers of the breast, ovary, and the intestinal tract, as well as other types of cancer.
- Anti-tumor antibiotics (*e.g.* doxorubicin, mitomycin C) interfere with enzymes

[11] http://www.cancer.gov/cancertopics/factsheet/Therapy/radiation (retrieved nov, 15 2012).

[12] http://www.cancer.org/treatment/treatmentsandsideeffects/treatmenttypes/chemotherapy/index (retrieved nov, 15 2012).

[13] http://www.cancer.org/treatment/treatmentsandsideeffects/treatmenttypes/chemotherapy/chemotherapyprinciplesanin-depthdiscussionofthetechniquesanditsroleintreatment/chemotherapy-principles-types-of-chemo-drugs (retrieved nov, 16 2012).

involved in DNA replication. These drugs work in all phases of the cell cycle. They are widely used for a variety of cancers. A dose-limiting side effect is the permanent heart damage.

- Mitotic inhibitors (*e.g.* paclitaxel, ixabepilone, vinblastine) are often plant alkaloids and other compounds derived from natural products. They can stop mitosis or inhibit enzymes from making proteins needed for cell reproduction. They work during the M phase of the cell cycle, but can damage cells in all phases. They are used to treat many different types of cancer including breast, lung, myelomas, lymphomas, and leukemias. These drugs can cause peripheral nerve damage.

Other types of cancer drugs are topoisomerase inhibitors (*e.g.* topotecan, etoposide), corticosteroids (*e.g.* prednisone, dexamethasone), antibodies (*e.g.* rituximab), and sex hormones or hormone-like drugs (tamoxifen).

The effectiveness of chemotherapy is often limited by toxicity to other tissues in the body. It is important to find a balance between killing the cancer cells and sparing the normal cells.

In cancer therapy it is common to combine the three different forms of therapy.

1.6 METAL-BASED CHEMOTHERAPEUTICS

The research of metal-based anticancer agents starts, when the physicist, Barnett Rosenberg in 1965, discovers the effect of cisplatin by serendipity.[14] The compound was first synthesized by Michele Peyrone in 1844, but he didn't know anything about its anti-carcinogenic effect.[15]

The original experiment of Rosenberg should have revealed the influence of an electric field on the cell division. For this, he used *Escherichia coli* bacteria in an ammonium chloride growing medium with two platinum electrodes. He noticed an abnormal, filamentary growth of the bacteria, and the inhibition of cell division.

Observation of oxidation of the platinum electrodes led him to the right interpretation.

[14] Rosenberg, B., VanCamp, L., and Krigas, T., *Nature*, **1965**, 205, 698-99.
[15] Peyrone, M., *Ann. Chem. Pharm. LI*, **1844**, 1-29.

The ammoniumhexachloroplatinat(IV)-complex, which was formed by chloride and ammonium ions in the medium, was converted to the cis-diamminetetrachloridoplatin(IV)-complex by photocatalytic reaction. The Pt^{IV} complex was further reduced under the reductive milieu of the bacteria to give the active cisplatin, which caused inhibition of cell division.[16]

Its antitumor activity was discovered (Rosenberg *et al*.1969) shortly thereafter.[17] Since its first approval in 1978, it has still remained the only antineoplastic agent with highly curative effects in a solid malignant tumor.[18] Cisplatin is particularly effective against cancers in the genito-urinary tract, and furthermore used in combination therapy for tumors of the ovaries, cervix, lung, lymphomas, bladder, head and neck, with promising results also on a series of other cancers.[19] Testicular cancer and its metastasis are cured almost 100% if detected early.[20] Prior to the application of cisplatin combination chemotherapy a cure rate of only 5-10% of advanced testicular cancer was achievable, today due to a synergistic effect approximately 80% of patients are disease free after treatment with cisplatin and other chemotherapeutics.[21]

The mode of action of cisplatin relies on the substitution of one or eventually both chlorido ligands by water molecules, followed by the reaction with DNA.[19] The distribution of the hydrolysis species depends on the pH and the chloride concentration. The lower intracellular chloride concentration favors hydrolysis and hence reactivity in intracellular environment.[19,20] DNA is the major pharmacological target of cisplatin and related platinum anticancer compounds. Binding to the DNA takes place in two steps, initial monofunctional binding, followed by bidentate coordination, leading to interstrand and especially intrastrand (90-95% of all adducts)[16] adducts (preferentially at guanine N7 position).[16,22] The helix axis becomes kinked, and undergoes unwinding, which results in apoptotic cell death.

However, only 1% (or less) of the administered cisplatin reaches the biological target DNA, the majority reacts with proteins and low molecular weight biomolecules, especially with those containing sulfur. This causes the high toxicity of cisplatin and its

[16] Galanski, M. and Keppler, B.K., *Pharm. Unserer Zeit*, **2006**, 35, 118-23.
[17] Rosenberg, B., VanCamp, L., Trosko, J.E., and Mansour, V.H., *Nature*, **1969**, 222, 385-6.
[18] Jakupec, M.A., Galanski, M., Arion, V.B., Hartinger, C.G., and Keppler, B.K., *Dalton Trans.*, **2008**, 183-94.
[19] Lippert, B., *BioMetals*, **1992**, 5, 195-208.
[20] Graf, N. and Lippard, S.J., *Adv. Drug Delivery Rev.*, **2012**, 64, 993-1004.
[21] Einhorn, L.H., *J Clin Oncol*, **1990**, 8, 1777-81.
[22] Marchan, V., Moreno, V., Pedroso, E., and Grandas, A., *Chem.--Eur. J.*, **2001**, 7, 808-15.

side effects like nephrotoxicity, nausea, bone-marrow suppression, and neurotoxicity.[19,20]

In the last years several thousand platinum coordination compounds have been prepared and tested for antitumor activity. Carboplatin shows less adverse side effects than cisplatin, due to the higher stability of the chelating 1,1-cyclobutanedicarboxylato ligand when compared to the chlorido ligands in cisplatin. No nephrotoxicity and a broader spectrum of activity are observed. Oxaliplatin is also active against cancer cell lines that are resistant to cisplatin and carboplatin, *e.g.* colon carcinomas.[23]

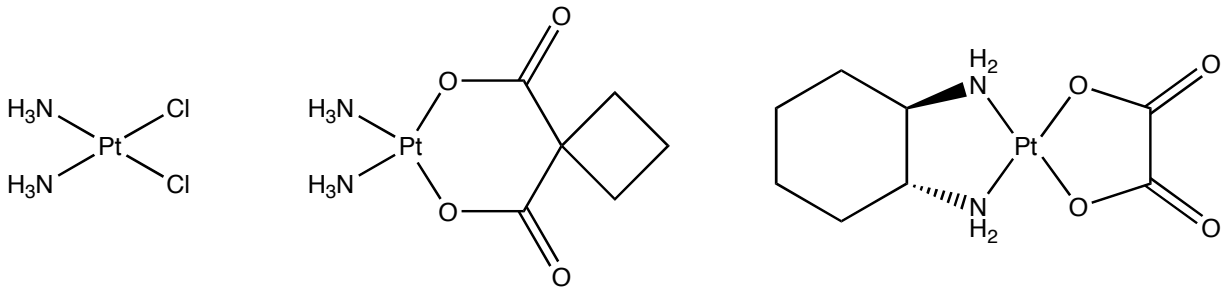

cisplatin carboplatin oxaliplatin

Figure 7: Platinum drugs in clinical use worldwide

Cisplatin, carboplatin and oxaliplatin (shown in Figure 7) are the only three platinum-based cancer chemotherapeutics in worldwide clinical use.[24] However, severe side effects and limited activity against several types of cancer limit their success. Drug resistance on tumor response, intrinsic or acquired, poses furthermore a great problem.[25]

An approach to overcome these limitations is the utilization of kinetically inert Pt^{IV} prodrugs that can be activated selectively by reduction at the tumor tissue, yielding the corresponding highly active Pt^{II} species upon the loss of both axial ligands.[20]

Nevertheless, the likelihood of discovering new drugs of this type with improved therapeutic properties must be regarded as extremely limited, and there is still a need for improved metal-based drugs, that clearly cannot mimic cisplatin in their mode of action Therefore a growing interest in non-platinum containing anticancer complexes has raised.

---

[23] Galanski, M.J., M.A.; Keppler, B.K., *Curr. Med. Chem.*, **2005**, 12, 2075-94.
[24] Gianferrara, T.B., I., Alessio, E., *Dalton Trans.*, **2009**, 7588-98.
[25] Heffeter, P., Jungwirth, U., Jakupec, M., Hartinger, C., Galanski, M., Elbling, L., Micksche, M., Keppler, B., and Berger, W., *Drug Resist Updat*, **2008**, 11, 1-16.

The non-platinum metal complexes, which are today in clinical progress are ruthenium, gallium, gold and arsenic compounds. Representatives with very promising results are NAMI-A (inhibition of metastasis), KP1019 (not only effective on metastasis, but also primary tumor), KP418, KP46, auranofin and As_2O_3.

1.6.1 RUTHENIUM BASED ANTI-CANCER DRUGS

Ruthenium complexes have attracted much interest as building blocks for new transition-metal-based anticancer agents. The unique properties of ruthenium make these compounds well suited for medicinal applications as an alternative to platinum anticancer drugs in the treatment of cancer cells resistant to cisplatin and its analogues. An advantage is the rate of ligand exchange, which is an important parameter for the biological activity. Ru^{II} and Ru^{III} show similar ligand exchange kinetics to those of Pt^{II} complexes. Furthermore, it is accessible in different oxidation states (II, III, IV) under physiological conditions. Other important features contributing to the promising expectation of ruthenium compounds are the ability of ruthenium to mimic iron, the availability of additional coordination sites in octahedral complexes and the altered shape of the complex.

Due to these characteristics, ruthenium compounds are often characterized as less toxic than platinum compounds[26] and offer the potential of a novel mode of action, the prospect of non-cross-resistance[27,28] and a different spectrum of activity.[24,29]

There are several hypotheses to explain its unique properties:

- **"Activation by reduction"** hypothesis proposed by Michael Clarke[29]

In biological systems, glutathione, ascorbate and single electron transfer proteins are able to reduce Ru^{III}, Ru^{IV} to the more active Ru^{II} species.

Solid tumors are often supplied with a poorly organized blood circulation and many parts receive an insufficient amount of oxygen.[26] This leads cells to prefer glycolysis instead of Kreb's cycle to produce energy; hence, the upregulation of glycolysis leads to microenvironmental acidosis.[30] The lower oxygen concentration, the higher glutathione

[26] Bergamo, A. and Sava, G., *Dalton Trans.*, **2011**, 40, 7817-23.
[27] Zeller, W.J., Fruhauf, S., Chen, G., Keppler, B.K., Frei, E., and Kaufmann, M., *Eur. J. Cancer*, **1991**, 27, 62-67.
[28] Coluccia, M., Sava, G., Loseto, F., Nassi, A., Boccarelli, A., Giordano, D., Alessio, E., and Mestroni, G., *Eur. J. Cancer*, **1993**, 29A, 1873-79.
[29] Clarke, M.J., *Coord. Chem. Rev.*, **2002**, 232, 69-93.
[30] Gatenby, R.A. and Gillies, R.J., *Nat. Rev. Cancer*, **2004**, 4, 891-99.

level, and the lower pH in cancer cells cause a strongly reducing environment.[31]

Therefore, an inert Ru^{III} prodrug can be applied, which is selectively activated by reduction at the altered physicochemical environment of the diseased site.

- **Iron mimicking**: Transportation of ruthenium to cancer cells by transferrin[32]

Ruthenium has a high affinity in binding to nitrogen and sulfur, which are found in many proteins, like transferrin or albumin. Transferrin is a protein that is involved in the transportation of iron and helps cells to get this essential element in a soluble way. Transferrin is useful for the metabolic process in which iron plays a role particularly during cell growth and division. Tumor cells have a fast cyclic activity and are rapidly dividing, and have therefore a greater requirement for iron. Expression of transferrin receptors on the cell surface of cancer cells is larger than on healthy ones.[33] When administered, the ruthenium-based anticancer drug should reveal a lower toxicity because less of the compound should reach healthy cells. Studies were reported that show that NAMI-A and KP1019 bind to transferrin.[34]

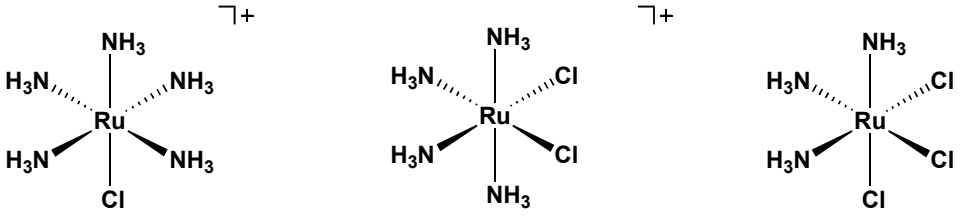

$[RuCl(NH_3)_5]$ *cis*-$[RuCl_2(NH_3)_4]$ *fac*-$[RuCl_3(NH_3)_3]$

Figure 8: First Ru^{II} and Ru^{III} compounds (M.J. Clarke, cisplatin as model)

First ruthenium-based anticancer agents (M.J. Clarke) derived from cisplatin are shown in Figure 8. The aim in the design is to cause DNA damage. Many ruthenium (II, III, IV) complexes with amine, dimethylsulfoxide, imine, polyaminopolycarboxylate, and N-heterocyclic ligands have been found to interact with DNA.[31] However, many of these complexes are barely soluble in aqueous solution, which is needed for intravenous administration. Solubility can be tuned by the adequate choice of the ligand sphere.

---

[31] Allardyce, C.S. and Dyson, P.J., *Platinum Met. Rev.*, **2001**, 45, 62-69.
[32] Som, P., Oster, Z.H., Matsui, K., Guglielmi, G., Persson, B.R.R., Pellettieri, M.L., Srivastava, S.C., Richards, P., Atkins, H.L., and Brill, A.B., *Eur. J. Nucl. Med.*, **1983**, 8, 491-4.
[33] Ryschich, E., Huszty, G., Knaebel, H.P., Hartel, M., Büchler, M.W., and Schmidt, J., *European Journal of Cancer* **2004**, 40, 1418-22.
[34] Messori, L., Vilchez, F.G., Vilaplana, R., Piccioli, F., Alessio, E., and Keppler, B., *Met.-Based Drugs*, **2000**, 7, 335-42.

The most prominent ruthenium-based anti-cancer drugs are NAMI-A and KP1019, which were the first ruthenium-based compounds to enter clinical trials and are now in clinical phase II study. Their structures are shown in Figure 9.

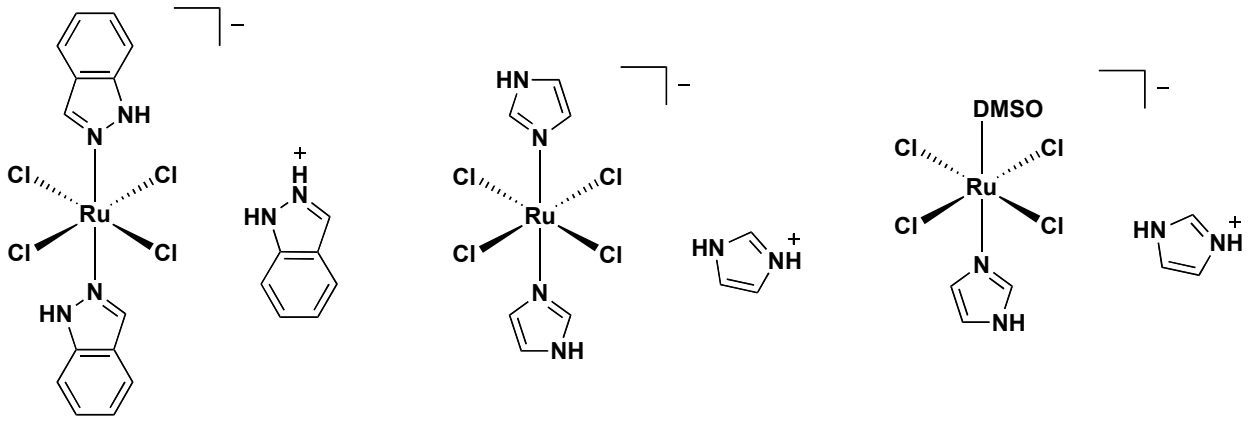

Figure 9: Developed ruthenium-based anticancer drugs (work: Keppler, Mestroni/Alessio)

Both metal center are in the oxidation state +III and have octahedral geometry.

According to Gianferrara and Coworkers[24] they belong to the group of functional compounds, where the metal has a functional role. The main interaction responsible for the activity is binding of the metal to the biological target. Functional compounds are mostly prodrugs that have to be activated first. A possible activation step is the chloride dissociation, maybe followed by reduction,[24] but still, the mechanism of action of NAMI-A and KP1019 and their biological target are not yet fully understood.

Their activity seems to be based on interactions with cell components different than DNA,[26] centering on interactions with mainly proteins, which seems to be extremely important for the anti-cancer activity of ruthenium compounds in general.[31]

KP1019 is cytotoxic to cancer cells, responsible for the activation of apoptosis through the mitochondrial pathway due to the interaction with molecules, which are important for the cell survival.[35] NAMI-A is relatively non-toxic, but is strongly effective against metastases, modifies cell invasion and prevents the spread of cancer.[36]

[35] Hartinger, C.G.J., M. A.; Keppler, B. K., *Chemistry&Biodiversity*, **2008**, 5, 2140-55.
[36] Yan, Y.K., Melchart, M., Habtemariam, A., and Sadler, P.J., *Chem. Commun.*, **2005**, 4764-76.

Due to the fact that the ruthenium (II) species is supposed to be the reactive species, responsible for the anticancer activity, the exploration of Ru^{II} compounds has raised lots of interest and much research has been carried out over the last decades. Of particular interest are the ruthenium (II) η^6-arene anticancer complexes, whereas the oxidation state +II of ruthenium is stabilized by the coordination of an aromatic moiety.

The ethylendiamine complexes and the RAPTA family are the most prominent representatives of this compound class and are at an advanced preclinical development stage[37], and will be discussed on the next pages.

Ruthenium-arene complexes are well suited for medicinal applications and are described to be immunosuppressant[38,39], nitric oxide scavengers[40], antimicrobial agents[41] and antimalarial[42].

Due to the coordination of ruthenium to an arene ligand, the metal is stabilized in its +II oxidation state. These ‘’half-sandwich” Ru^{II} (arene) complexes retain good aqueous solubility which is an advantage for their clinical use. Furthermore, the arene ligand is relatively inert towards displacement under physiological conditions.[36] The complexes form the so-called ‘’piano-stool’’ structure, where the arene forms the seat of the piano-stool and the ligands represent the legs (see Figure 10). Using a chelating ligand that binds to Y and Z seems to increase anticancer activity next to stability.

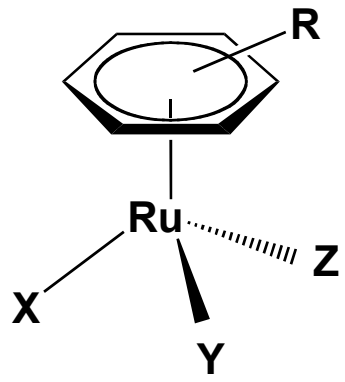

Figure 10: „Piano-stool“-configured ruthenium (II) arene complex

[37] Süss-Fink, G., *Dalton Trans.*, **2010**, 39, 1673-88.
[38] Dwyer, D.S., Gordon, K., and Jones, B., *Int. J. Immunopharmacol.*, **1995**, 17, 931.
[39] Clarke, M.J., Bailey, V., Doan, P., Hiller, C., LaChanceGalang, K.J., Daghlian, H., Mandal, S., Bastos, C.M., and Lang, D., *Inorg. Chem.*, **1996**, 35, 4896.
[40] Hayton, T.W., Legzdins, P., and Sharp, W.B., *Chem. Rev.*, **2002**, 102, 935.
[41] Allardyce, C.S., Dyson, P.J., Ellis, D.J., Salter, P.A., and Scopelliti, R., *Journal of Organometallic Chemistry*, **2003**, 668, 35-42.
[42] Sánchez-Delgado, R.A., Navarro, M., Pérez, H., and Urbina, J.A., *J Med Chem*, **1996**, 39, 1095-99.

By changing the three main building blocks of the piano-stool complex, the pharmacological properties can be improved and fine-tuned. The remaining monodentate ligand X, which acts as the leaving group (often a chloride), can be important to control the activation timing. The bidentate ligand YZ helps to control stability and ligand-exchange kinetics. The arene stabilizes the metal in its +II oxidation state and helps furthermore to influence cell uptake and interactions with potential targets.[36]

The anticancer activity of $[(\eta^6\text{-arene})Ru(en)(Cl)]^+$ compounds and the influence of the coordinated arene has been investigated and it was found that the activity depends on the size of the coordinated arene (ben < Cp (cym) < bip < DHA < THA. The structures of the investigated arenes are shown in Figure 11.

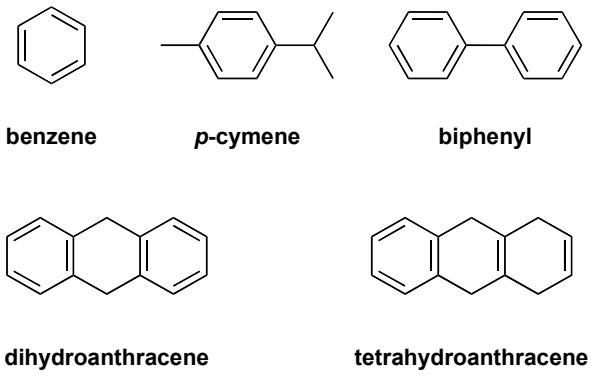

Figure 11: Structures of some coordinated arenes in "piano-stool" complexes

The utilization of hydrophobic arenes, a chelating non-leaving ligand, and one leaving group results in high cytotoxicity.[36]

Ruthenium(II) – arene complexes are active against a wide spectrum of cancer cells, *e.g.* $[(\eta^6\text{-DHA})Ru(en)\text{-}Cl]PF_6$ and $[(\eta^6\text{-bip})Ru(en)\text{-}Cl]PF_6$ are active against HT29 colon, Panc-1 pancreatic and NXO2 lung cancer cells with IC_{50} values in the µM range.[36,43]

The mechanism of action is different than the one of Ru^{III} complexes. The first step seems to be the chloride ligand exchange by a water molecule leading to the more active aqua complex. The ruthenium(II) – arene (en) complexes show a faster rate of exchange than cisplatin. The ligand exchange reactions can be influenced by the arene ligand, restricted on its steric and electronic effects. The equilibrium constants for aquation are small, hence at a physiologically-relevant concentration of the Ru^{II} arene

[43] Habtemariam, A., Melchart, M., Fernández, R., Parsons, S., Oswald, I.D.H., Parkin, A., Fabbiani, F.P.A., Davidson, J.E., Dawson, A., Aird, R.E., Jodrell, D.I., and Sadler, P.J., *Journal of Medicinal Chemistry*, **2006**, 49, 6858-68.

complexes (0.5 – 5 µM), the complex should exist in blood plasma mostly as the less reactive chlorido species (> 89%), whereas in the nucleus (where the chloride concentration is about 4 mM [44,45] a significantly larger amount (45 – 65%) of the reactive aqua species is present. Since the coordinated aqua ligand undergoes acid dissociation, the less reactive hydroxido species is formed. The dominant species for cisplatin (pK_a = 6.56 for the monoaqua species)[46] in the cell nucleus is the less reactive hydroxo form,[36] whereas ruthenium complexes which have higher pK_a values (for (η^6-arene) Ru(en)(H_2O)]$^{2+}$ around 8), only a smaller amount of OH-species is found at biologically pH 7.2 – 7.4 in the cell nucleus.[36]

Manipulating the rate and extent of aquation, and the pK_a value of coordinated water can even optimize their efficacy. This can be done by changing the chelating ligand. When a stronger electron donor, *e.g.* acac, is used instead of en, a higher resulting pK_a value is the consequence.[47]

Direct coordination to the bases, intercalation, and stereospecific hydrogen bonding are important characteristics to include in the design of Ru^{II} arene complexes to optimize the recognition of DNA.[36]

Sadler *et al*.[36] studied the interaction of Ru^{II} arene complexes (with the general formula [(η^6-arene)Ru(en)Cl]$^+$) with oligonucleotides and DNA. The complexes bind selectively to G bases on DNA oligonucleotides, forming mono- and diruthenated adducts (as shown by LC-ESI-MS experiments). The presence of cytochrome-c and L-histidine has no effects on that interaction, and no corresponding adducts are observed, it is suggested that the favored reaction site of [(η^6-arene)Ru(en)Cl]$^+$ complexes in cells is DNA (or RNA).

In a mononucleoside-binding-study, the preferred binding site of these ruthenium (II) arene complexes seems to be N7 of guanosine (G), showing the following order of affinity: G(N7) > T(N3) > C(N3) > A(N7), A(N1), and therefore leading to the presumption that these complexes target selectively G rich regions of DNA, such as telomers, which play key roles in cell division. The same pattern of site selectivity is shown for mononucleotides, whereby metallation of N7 in guanosine causes significant electronic perturbations at N1H, which is a hydrogen-bond donor in G-C base pairs in

[44] Jennerwein, M. and Andrews, P.A., *Drug Metab. Dispos.*, **1995**, 23, 178.
[45] Lippert B., Cisplatin: Chemistry and Biochemistry of a Leading Anticancer Drug, **1999**.
[46] Andersson, A., Hedenmalm, H., Elfsson, B., and Ehrsson, H., *J. Pharm. Sci.*, **1994**, 83, 859-62.
[47] Hasegawa, T., Lau, T.C., Taube, H., and Schaefer, W.P., *Inorg. Chem.*, **1991**, 30.

the DNA double helix, and may as a result influence the stability of the double helix. The nature of the chelating ligand can influence this nucleobase-binding preference, *e.g.* the en ligand exhibits a particularly high preference of G-binding due to further strong hydrogen-bond interactions, whereas the acac ligand prevents the favorable interaction by steric restrictions and in that case the affinity in binding G(N7) is same with A(N7).

Circular dichroism and differential pulse polarography studies show that the bip and anthracene complexes cause non-denaturational changes in DNA conformation (like cisplatin), whereas cym complexes distort the DNA more severely (like transplatin).[48] Intercalation and/or minor groove binding to CT-DNA are observed for bip and anthracene derivatives, but not for cym.

However, all these Ru^{II} arene complexes (bip, DHA, THA or cym) cause bending of DNA.

Further studies on DNA duplexes revealed information about a different mechanism of action. Observation that the activity of [Ru^{II} (en) arene] complexes does not involve recognition of their distorted DNA adducts by HMG domain proteins as a crucial step (as it is in the case of cisplatin and its direct adducts)[36], and that a different remove (other than nucleotide excision repair, which causes cisplatin resistance) of these compounds occurs, states a different mechanism of antitumor activity of Ru^{II} arene complexes.

Ru^{II} arene complexes have shown to react with amino acids and proteins as well. Their affinity in binding is L-Cys > L-Met > L-His. Studying the reactivity towards these amino acids is interesting in terms of finding the protein targets, understanding detoxification and resistance mechanisms.[49] Although reactions with amino acids and proteins occur, their reactivity compared to DNA is low; this could be the reason for the low toxic side effects of such complexes.[50] However, the weak binding can promote transport and delivery to cancer cells.

Among the best-studied and most promising ruthenium(II) – arene ‘’piano-stool’’ anticancer compounds are furthermore the RAPTA-type complexes.

RAPTA compounds are characterized by a monodentate 1,3,5-triaza-7-phosphatricyclo[3.3.1.1]decane (PTA) ligand, a η^6-arene ligand bound to the metal

[48] Brabec, V. and Novakova, O., *Drug Resist. Updates*, **2006**, 9, 111-22.
[49] Reedijk, J., *Proc. Natl. Acad. Sci.*, **2003**, 100.
[50] Aird, R.E., Cummings, J., Ritchie, A.A., Muir, M., Morris, R.E., Chen, H., Sadler, P.J., and Jodrell, D.I., *Br. J. Cancer*, **2002**, 86, 1652.

center, and two remaining sites for the leaving groups, usually chlorides: [Ru(η^6-arene)Cl_2(PTA)]. As the PTA ligand is hydrophilic the complexes possess good aqueous solubility.[51]

A known example is the *p*-cymene derivative, RAPTA-C, which has activity against, for example, SK-N-SH neuroblastoma cells, and induces apoptosis in nanomolar concentrations, see Figure 12.[31]

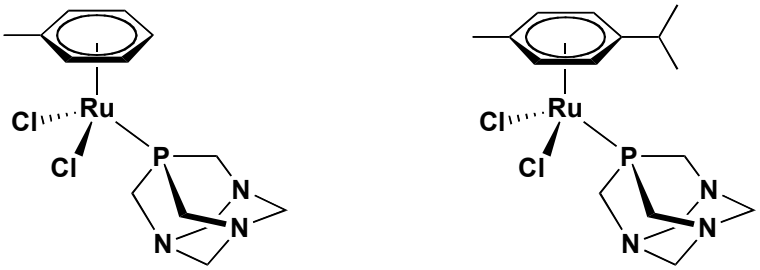

RAPTA-T RAPTA-C

Figure 12: Structure of RAPTA complexes

Usually, the RAPTA compounds are weakly cytotoxic *in vitro*, but show selective antimetastatic activity *in vivo*. RAPTA-T (Figure 12) is more effective on highly invasive cancer cells than on less invasive cell lines; it interferes with metastatic progression;[52,53] *e.g.* it reduces the primary tumor (MCa, mammary carcinoma) only modestly, but inhibits selectively the development and growth of lung metastases.[51]

Furthermore, they interact strongly with proteins, and are able to discriminate binding to different proteins, but show a relatively low tendency to bind DNA. This may be due to the hydrophobic arene moiety and can be the reason for the antimetastatic action.[51] Nevertheless they are able to induce DNA damage; *e.g.* RAPTA-C shows a pH dependent DNA damage.[54] Only at a reduced pH (< 7) DNA damage is observed. Thus, considering the existing hypoxia in cancer cells, a selective anticancer action is expected. Furthermore, it is more reactive with dGMP, when the pH is reduced from 7.4 to 6.[55]

[51] Ang, W.-H., Casini, A., Sava, G., and Dyson, P.J., *J. Organomet. Chem.*, **2011**, 696, 989-98.
[52] Dyson, P.J., *Chimia*, **2007**, 61.
[53] Bergamo, A., Masi, A., Dyson, P.J., and Sava, G., *Int. J. Oncol.*, **2008**, 33, 1281.
[54] Allardyce, C.S., Dyson, P.J., Ellis, D.J., and Heath, S.L., *Chem. Commun.*, **2001**, 1396.
[55] Groessl, M., Hartinger, C.G., Dyson, P.J., and Keppler, B.K., *J. Inorg. Biochem.*, **2008**, 102, 1060.

The RAPTA structure is quite stable under physiological conditions, and studies have shown that aquation of the chloride bonds seems not to be essential for the anticancer drug activity, although it is likely to occur following cellular uptake. Due to the favorable physicochemical properties of RAPTA compounds and their highly promising antitumor and antimetastatic properties, the structure reveals an ideal scaffold for rational drug design.

Many additional novel ruthenium(II)-arene compounds for drug delivery and therapy are in progress and are showing promising advances. Compounds, which show strong binding to a protein kinase, Pim-1, have been developed.[56,57,58] Furthermore, water solubility of paullones, which are potent cyclin-dependent kinase (CDK) and glycogen synthase kinase-3 inhibitors and limited by their low water solubility, can be increased by coordination to ruthenium(II)- and osmium(II)- arene moieties.[59,60,61] Another approach are the pyridone- based dinuclear ruthenium(II)-arene complexes connected *via* an alkyl chain, which are highly active in a colorectal carcinoma cell line, but inactive in the form of the mononuclear complex.[62,63,64] The cytotoxic activity depends on the spacer length between the metal centers;[62,65] and multiple ruthenium(II) – arene units bound to a dendritic polypyridyl core also showed promising results.[66]
As shown, there are limitless strategies and approaches in drug design, which open the way for a promising future development.

---

[56] Bregman, H., Carroll, P.J., and Meggers, E., *J. Am. Chem. Soc.*, **2006**, 128, 877.
[57] Debreczeni, J.E., Bullock, A.N., Atilla, G.E., Williams, D.S., Bregman, H., Knapp, S., and Meggers, E., *Angew. Chem. Int. Ed. Engl.*, **2006**, 45, 1580.
[58] Maksimoska, J., Feng, L., Harms, K., Yi, C.L., Kissil, J., Marmorstain, R., and Meggers, E., *J. Am. Chem. Soc.*, **2008**, 130, 15764.
[59] Schmid, W.F., John, R.O., Arion, V.B., Jakupec, M.A., and Keppler, B.K., *Organometallics*, **2007**, 26, 6643.
[60] Schmid, W.F., John, R.O., Mühlgassner, G., Heffeter, P., Jakupec, M.A., Galanski, M., Berger, W., Arion, V.B., and Keppler, B.K., *J. Med. Chem.*, **2007**, 50, 6343.
[61] Schmid, W.F., Zorbas-Seilfried, S., John, R.O., Arion, V.B., Jakupec, M.A., Roller, A., Galanski, M., Chiorescu, I., Zorbas, H., and Keppler, B.K., *Inorg. Chem.*, **2007**, 46, 3645.
[62] Mendoza-Ferri, M.G., Hartinger, C.G., Eichinger, R.E., Stolyarova, N., Severin, K., Jakupec, M.A., Nazarov, A.A., and Keppler, B.K., *Organometallics*, **2008**, 27, 2405.
[63] Mendoza-Ferri, M.G., Hartinger, C.G., Mendoza, M.A., Groessl, M., Egger, A.E., Eichinger, R.E., Mangrum, J.B., Farrell, N.P., Maruszak, M., Bednarski, P.J., Klein, F., Jakupec, M.A., Nazarov, A.A., Severin, K., and Keppler, B.K., *J. Med. Chem.*, **2009**, 52, 916.
[64] Mendoza-Ferri, M.G., Hartinger, C.G., Nazarov, A.A., Eichinger, R.E., Jakupec, M.A., Severin, K., and Keppler, B.K., *Organometallics*, **2009**, 28, 6260.
[65] Mendoza-Ferri, M.G., Hartinger, C.G., Nazarov, A.A., Kandioller, W., Severin, K., and Keppler, B.K., *Appl. Organometal. Chem.*, **2008**, 22, 326-32.
[66] Govender, P., Antonels, N.C., Mattsson, J., Renfrew, A.K., Dyson, P.J., Moss, J.R., Therrien, B., and Smith, G.S., *J. Organomet. Chem.*, **2009**, 694, 3470.

Replacement of the metal center with homologs of the same group leads to isostructural complexes with small changes of the geometrical parameters, but significant differences in terms of kinetics (heavier metals are substantially more inert) and redox potential.[24]

1.6.2 OSMIUM AND RHODIUM-BASED ANTICANCER AGENTS

Other metals of the platinum group have been assigned to exhibit anticancer activity but were not that much investigated so far. Osmium-based anticancer agents attracted interest only in the last years and various complexes with different mono- and bidentate ligands were investigated towards their antiproliferative potential (see Figure 13). Osmium offers similar to ruthenium a wide range of accessible oxidation states under physiological conditions (II, III, IV).

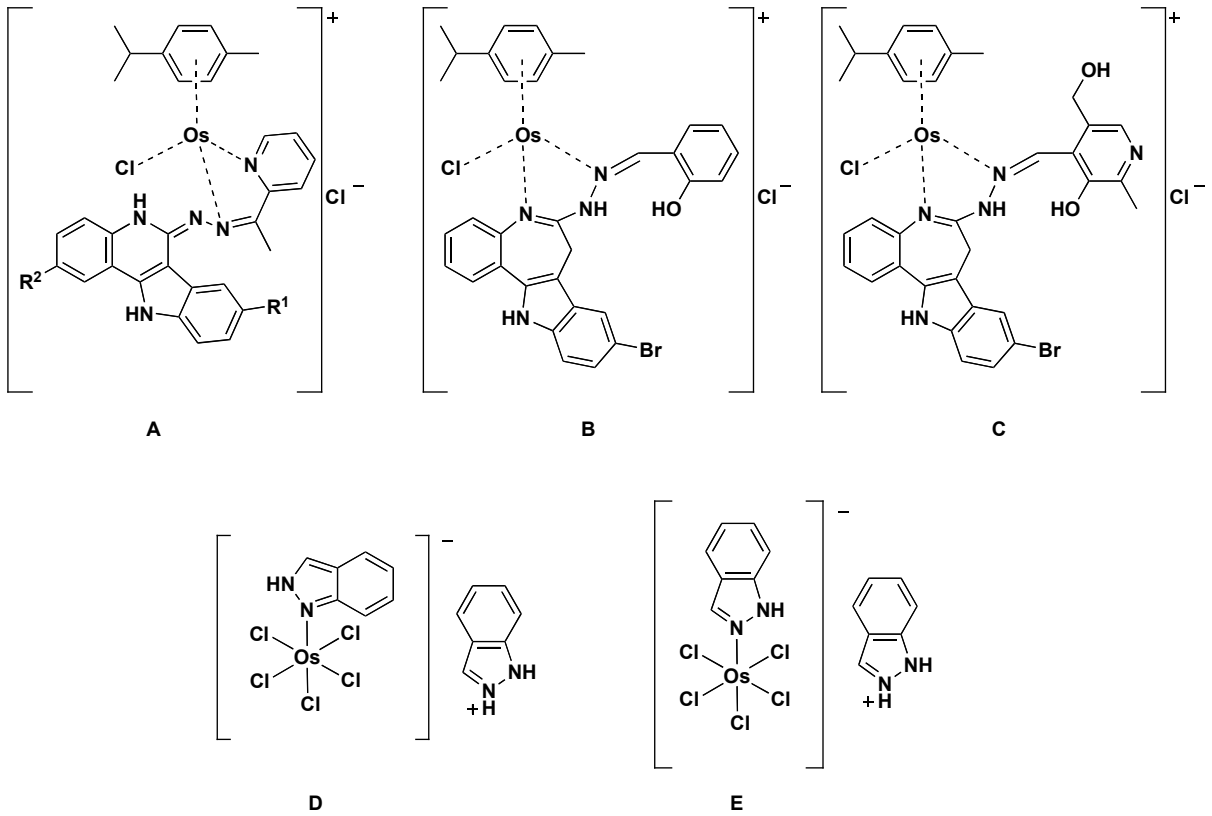

Figure 13: Osmium-arene complexes of indoloquinolines with R^1, R^2 H, CH_3, Cl, Br (A)[67], or modified paullones (B and C)[68], and some Os^{IV} complexes with indazoles-ligands (D and E)[69].

The first notation of the anticancer properties of rhodium $RhCl_3 \cdot H_2O$ was in 1953[70], but not a lot of research followed. The pseudo first-order rate constant for water exchange

[67] Filak, L.K., Goeschl, S., Hackl, S., Jakupec, M.A., and Arion, V.B., *Inorg. Chim. Acta*, **2012**, 393, 252-60.
[68] Muehlgassner, G., Bartel, C., Schmid, W.F., Jakupec, M.A., Arion, V.B., and Keppler, B.K., *J. Inorg. Biochem.*, **2012**, 116, 180-87.
[69] Buechel, G.E., Stepanenko, I.N., Hejl, M., Jakupec, M.A., Keppler, B.K., Heffeter, P., Berger, W., and Arion, V.B., *J. Inorg. Biochem.*, **2012**, 113, 47-54.

by the octahedral hexaaqua cation $[Rh(H_2O)_6]^{3+}$ is about 4 orders of magnitude lower than that for the squareplanar $[Pt(H_2O)_4]^{2+}$ cation.[71] Because of this kinetic inertness, but also their high general toxicity, and low solubility, rhodium complexes have until recently thought not to be suitable for further investigations in the means of drug design. Metallointercalators are another novel approach for ruthenium, osmium and rhodium metal-based complexes. Figure 14 shows octahedral rhodium complexes, and also one ruthenium complex containing multi-heterocyclic aromatic ligands such as phen, phi, dppz, phzi and eilatin.[72,73,74]

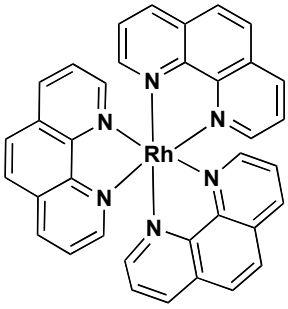

$[Rh(phen)_3]^{3+}$

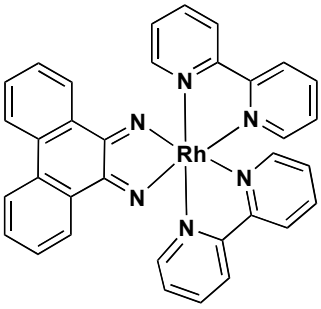

$[Rh(bpy)_2phi]^{3+}$

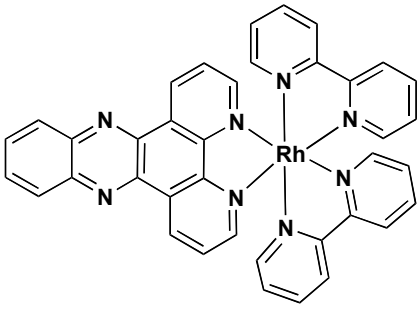

$[Rh(bpy)_2dppz]^{2+}$

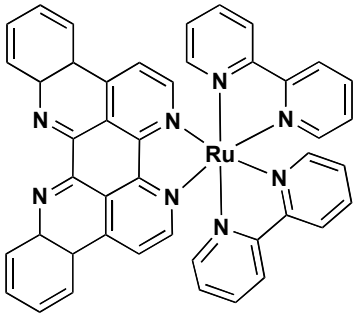

$[Ru(bpy)_2eilatin]^{2+}$

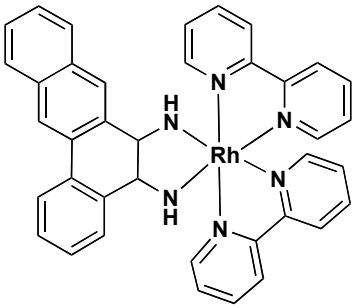

$[Rh(bpy)_2phzi]^{3+}$

Figure 14: Structures of some octahedral rhodium and a ruthenium metallointercalator

Metallointercalators are characterized to exhibit a dual function: they bind to DNA both by metal coordination and through intercalation of the attached aromatic ligands. They have shown a better potential towards cancer cells, than their nonintercalating analogues (Ru-bip and Ru-THA than Ru-*p*-cym or Ru-ben)[36]. Their dual function leads

---

[70] Geldmacher, Y., *Inorganica Chimica Acta*, **2012**, 393, 84-102.
[71] Helm, L. and Merbach, A.E., *Coord. Chem. Rev.*, **1999**, 187, 151-81.
[72] Zeglis, B.M., Pierre, V.C., and Barton, J.K., *Chem. Commun.*, **2007**, 4565-79.
[73] Elias, B. and Kirsch-De Mesmaeker, A., *Coord. Chem. Rev.*, **2006**, 250, 1627-41.
[74] Luedtke, N.W., Hwang, J.S., Nava, E., Gut, D., Kol, M., and Tor, Y., *Nucleic Acids Res.*, **2003**, 31, 5732-40.

to unusual DNA distortions and novel mechansims of biological activity, which affects recognition by DNA binding proteins and repair enzymes and hence induces apoptosis.[75]

By combining the use of one or more ligands with a stronger *trans* effect and the coordination of ligands that are themselves cytotoxic, it is hoped to improve anticancer activity. In the case of rhodium, octahedral Rh^{III} complexes with polypyridyl and other aromatic chelates have shown to exhibit high cytotoxicity and in certain cases promising relative tolerance by healthy cells. Polypyridyl ligands (pp) are themselves cytotoxic and there is a growing interest in the use of these compounds as DNA intercalators or groove binders.[76] The use of an anionic arene ligand for example Cp* shows a highly labilizing effect on the remaining aqua ligands, which is not observed in the case of neutral arenes, like benzene, *p*-cym. Polypyridyl complexes of the type $[(\eta^6\text{-Cp*})RhCl(pp)]^+$ undergo rapid aquation due to the strong trans effect of the anionic $[Cp^*]^-$ ligand.[70]

1.7 BIOACTIVE LIGANDS

One approach of preparing multi-targeted compounds is the combination of anticancer metal complexes with bioactive ligands, as reported for ethacrynic acid, flavonol derivatives and others.[77,78,79] Lapachol (2-hydroxy-3-(3-methylbut-2-en-1-yl)naphthalene-1,4-dione) and flavonols share the same 5-membered coordination motif of *O,O*-bidentate anionic ligands as also observed for hydroxypyr(id)ones used in medicinal chemistry.[80] Furthermore, lapachol has antibiotic and anticancer properties and was investigated in clinical trials as an anticancer agent.[81,82] Its mode of action is supposed to be related to the generation of reactive oxygen species (ROS), which harm

[75] Liu, H.-K. and Sadler, P.J., *Acc. Chem. Res.*, **2011**, 44, 349-59.
[76] Erkkila, K.E., Odom, D.T., and Barton, J.K., *Chem. Rev.*, **1999**, 99, 2777-95.
[77] Chatterjee, S., Biondi, I., Dyson, P., and Bhattacharyya, A., *JBIC Journal of Biological Inorganic Chemistry*, **2011**, 16, 715-24.
[78] Kurzwernhart, A., Kandioller, W., Bartel, C., Bachler, S., Trondl, R., Muhlgassner, G., Jakupec, M.A., Arion, V.B., Marko, D., Keppler, B.K., and Hartinger, C.G., *Chemical Communications*, **2012**, 48, 4839-41.
[79] Filak, L., Mühlgassner, G., Jakupec, M., Heffeter, P., Berger, W., Arion, V., and Keppler, B., *Journal of Biological Inorganic Chemistry*, **2010**, 15, 903-18.
[80] Kandioller, W., Kurzwernhart, A., Hanif, M., Meier, S.M., Henke, H., Keppler, B.K., and Hartinger, C.G., *Journal of Organometallic Chemistry*, **2011**, 696, 999-1010.
[81] Edvaldo Rodrigues, d.A., *The Open Natural Products Journal*, **2009**, 2, 42-47.
[82] Hussain, H.K., Karsten; Ahmad, Viqar Uddin; Miana, Ghulam Abbas; Green, Ivan Robert *ARKIVOC*, **2007**, 2, 42-47.

DNA and subsequently induce apoptosis, and biologically active Bi and Sb complexes were reported recently.[83,84]

Active organometallic Ru^{II}(arene) complexes have clearly emerged as highly promising alternatives to overcome the disadvantages of clinically-used platinum drugs.[85] Therefore, the combination of bioactive lapachol with an organometallic moiety is a promising strategy with the metal center altering the chemical and biological properties of the ligand.

1.7.1 NAPHTHOQUINONES

Naphthoquinones are naturally occurring secondary plant metabolites, which display a broad spectrum of pharmacological properties. They belong to a class of organic compounds derived from naphthalene. Three isomers are normally discussed: 1,2-naphthoquinone, 1,4-naphthoquinone and 2,6-naphthoquinone (*amphi*-naphthoquinone), depending on the position of the carbonyl group. The most prominent examples for 1,4-naphthoquinones are the vitamin K derivatives.

Compounds bearing a quinone moiety have promising biological activity. It has been reported that naphthoquinones can generate “reactive oxygen species” that can damage cells.[81] Due to this quinone scaffold, they are able to generate semiquinone radicals by bioreduction, and subsequently induce oxidative stress. They are known to interfere with the bioactivities of enzymes known as topoisomerases, which are critical for DNA replication in cells.

There is a growing interest in the investigation of pharmacology and the mode of action of these substances.[81]

[83] Parrilha, G., Vieira, R., Campos, P., Silva, G., Duarte, L., Andrade, S., and Beraldo, H., *BioMetals*, **2012**, 25, 55-62.

[84] Oliveira, L.G.d., Silva, M.M., Paula, F.C.S.d., Pereira-Maia, E.C., Donnici, C.L., Simone, C.A.d., Frézard, F., Júnior, E.N.d.S., and Demicheli, C., *Molecules*, **2011**, 16, 10314-23.

[85] Hartinger, C.G., Metzler-Nolte, N., and Dyson, P.J., *Organometallics*, **2012**, 31, 5677-85.

Lapachol[81]

Lapachol was first isolated by E. Paterno from *Tabeuia avellanedae* (Bignoniaceae) in 1882, and it can furthermore be found in other families such as Verbenaceae, Proteaceae, Leguminosae, Sapotaceae, Scrophulariaceae, and Malvaceae.[81]

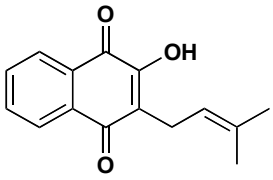

Figure 15: Structure of lapachol

Lapachol, structure shown in Figure 15, and its derivatives have been described to exhibit the following therapeutic activities:

Antitumor activity: A study in 1980 shows that lapachol is able to shrink tumors and reduce feeling of pain and remit tumors completely of three patients with various cancers (liver, kidney, breast, prostate and cervix). The antitumor activity seems to be due the interaction of lapachol with nucleic acids, and a further interaction between base pairs of the DNA helix causing the inhibition of DNA replication and RNA synthesis. Because of its anticancer activity it is interesting to search further for developed analogs with improved activity. Lots of synthetic analogs have been investigated, but only some have been found to be active, see Figure 16.

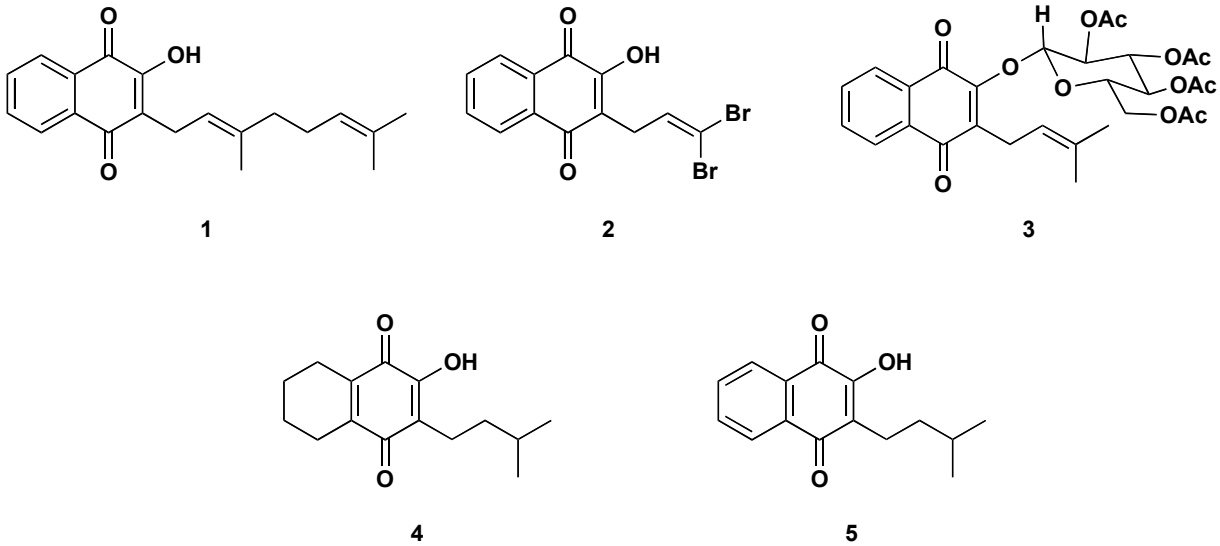

Figure 16: Lapachol derivatives showing biological activity

2-(3,7-dimethyl-2,6-octadienyl)-3-hydroxy-1,4-naphthoquinone (**1**) and 2-(3',3'-dibromo-2-propenyl)-3-hydroxy-1,4-naphthoquinone (**2**) are active against the Walker 256 tumor

cell line, 2-(3'-methyl-2-butenyl)-3-tetraacetyl-*β*-D-glucopyranosyloxy)-1,4-naphthoquinone (**3**) increased the life span by over 80% in mice inoculated with leukemic cells. Recently two lapachol derivatives (**4**, **5**) have shown to be active against lung, breast, melanoma, ovarian, prostate, and renal cancer.[83]

Anti-metastatic activity: Lapachol was found to possess anti-metastatic potential *in vivo*, and is able to induce alterations in the protein profile in the human HeLa cancer cell line where it inhibits cellular invasiveness.

Leishmanicidal activity: How exactly lapachol can induce lysis of intracellular amastigotes *in vitro* is not yet clear. However, it is known, that naphthoquinones in general (especially lapachol and *β*-lapachone) interfere with the oxygen metabolism of the cancer cell, and block so respiration and generate free oxygen radicals. After all, it seems, that the most important metabolite involved in leishmania killing in mice is nitric oxide, which is produced due to the induction of nitric oxide synthetase by IFN-γ.

Lastly a broad range of other biological activities have been attributed to lapachol: miscellaneous activities: antioxidant, cytotoxic (in human Promyelocytic Leukemia HL-60 cell line), analgesic, and antipsoriatic activity; anti-abscess, anticarcinomic, anti-edemic, anti-inflammatory, antimalarial, antiseptic, antitumor, antiviral, bactericidal, fungicidal, insectifugal, pesticidal, protisticidal, respiradepressant, schistosomicidal, termiticidal, and viricidal.[83]

Niehues *et al.*[86] gave first insights into the oxidative metabolism of lapachol by an *in vitro* biomimetic model with Jacobsen catalyst (manganese(III)salene) and iodosylbenzene as oxidizing agent. Eleven oxidation products were formed, whereby two competitive oxidation pathways were postulated; these *in vitro* derivatives were used to identify the resulting metabolites in *in vivo* samples by GC-MS (SIM mode). Two metabolites were found in Wistar rats' plasma after oral administration of lapachol: α-lapachone and dehydro-α-lapachone. α-lapachone is proposed to be already formed during the acidic gastric passage and thereupon absorbed, whereas the genuine oxidation metabolite dehydro-α-lapachone seems to be formed by cytochrome P450 enzymes mediated catalysis. Oxidation by Jacobsen catalyst model, using an

[86] Niehues, M., Barros, V.P., Emery, F.d.S., Dias-Baruffi, M., Assis, M.d.D., and Lopes, N.P., *Eur. J. Med. Chem.*, **2012**, 54, 804-12.

oxomanganese(V) complex as oxygen transfer agent, can mimic certain reactions of cytochrome P450, and therefore predict and elucidate *in vivo* phase I metabolism.

Lapachol has been reported as a biological active compound, and its efficacy as an antineoplastic agent has been confirmed. However, in 1974, the National Cancer Institute terminated further studies on the action of lapachol as an antineoplastic agent, due to the high concentrations, which are necessary for an effective therapy and the very toxic side effects. Studies of new and novel lapachol analogues should follow to ensure a promising development of this potentially potent biological molecule.

Compound 5 (Cpd 5)[87]

Vitamin K3 (Figure 17), its synthetic derivative menadione, and its analogues are currently attracting much attention. They have been shown to have anticancer activity against a series of tumor cell lines.[88]

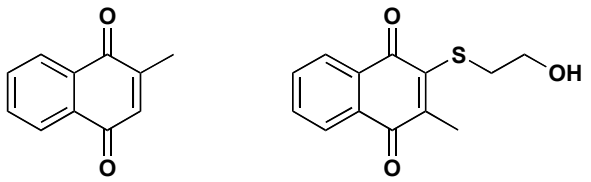

Vitamin K3 menadione

Compound 5

Figure 17: Structures of Vitamin K3 and its derivative Compound 5

The main function of K vitamins is to act as co-factors for γ-glutamyl carboxylase. However, it has been recently shown that they can inhibit cell growth. Lots of research in different synthetic K vitamin analogues with various side chains has been done in the last decade. Especially analogues with short thio-ethanol side chains have been found to be highly potent growth inhibitors of various tumor cell lines *in vitro*; Cpd 5 (2-(2-mercaptoethanol)-3-methyl-1,4-naphthoquinone) being one of the most potent growth inhibitors and apoptosis inducers in several tumor cell lines *in vivo* and *in vitro*[89] is shown in Figure 17. It is thought that the growth inhibition is regulated by sulfhydryl arylation of cellular glutathione and cysteine-containing proteins and not by oxidative stress. The protein tyrosine phosphatases (PTPs), which contain a cysteine at their catalytic site, are proteins that regulate mitogenic signal transduction and cell cycle

[87] Carr, B.I., Wang, Z., and Kar, S., *J. Cell. Physiol.*, **2002**, 193, 263-74.
[88] Chen, C., Liu, Y.-Z., Shia, K.-S., and Tseng, H.-Y., *Bioorg Med Chem Lett*, **2002**, 12, 2729-32.
[89] Chen, L., *Guoji Zhongliuxue Zazhi*, **2009**, 36, 491-94.

progression. Inhibition by Cpd 5 induces prolonged tyrosine phosphorylation and activation of several kinases and transcription factors including EGFR, ERK1/2, and Elk1, whereby prolonged ERK1/2 phosphorylation strongly correlates with Cpd 5-mediated growth inhibition. Cpd 5 has been shown to be especially a potent, selective, and partially competitive inhibitor of Cdc25 phosphatases resulting in the inhibition of cell cycle progression and leading to cell growth arrest.

Cpd5 is furthermore capable of inhibiting CREB (cAMP response element-binding protein) and phosphorylation of pp90RSK, which reduces the expression of genes mediated by cAMP response element and cell growth. Additionally, Cpd 5 activates the caspase pathway and induces apoptosis.[89]

Cpd 5 is able to arrest cell cycle progression at both G_1 and G_2-M. This novel vitamin K analogue could be interesting for cell cycle control studies and its promising pharmacophore may contribute to further development of drug design and novel anticancer agents.[90]

[90] Tamura, K., Southwick, E.C., Kerns, J., Rosi, K., Carr, B.I., Wilcox, C., and Lazo, J.S., *Cancer Res*, **2000**, 60, 1317-25.

2 RESULTS AND DISCUSSION

2.1 STUDIES ON NOVEL *O,S* – CHELATES

2.1.1 SYNTHESIS OF THE LIGANDS

One part of this master thesis was the synthesis of compound 5 derivatives as novel naphthoquinone-based *O,S*-chelates. In general, the substances were obtained by conversion of the 1,4-naphthoquinone precursor with different sulfhydryl group containing reagents *via* Michael-addition.

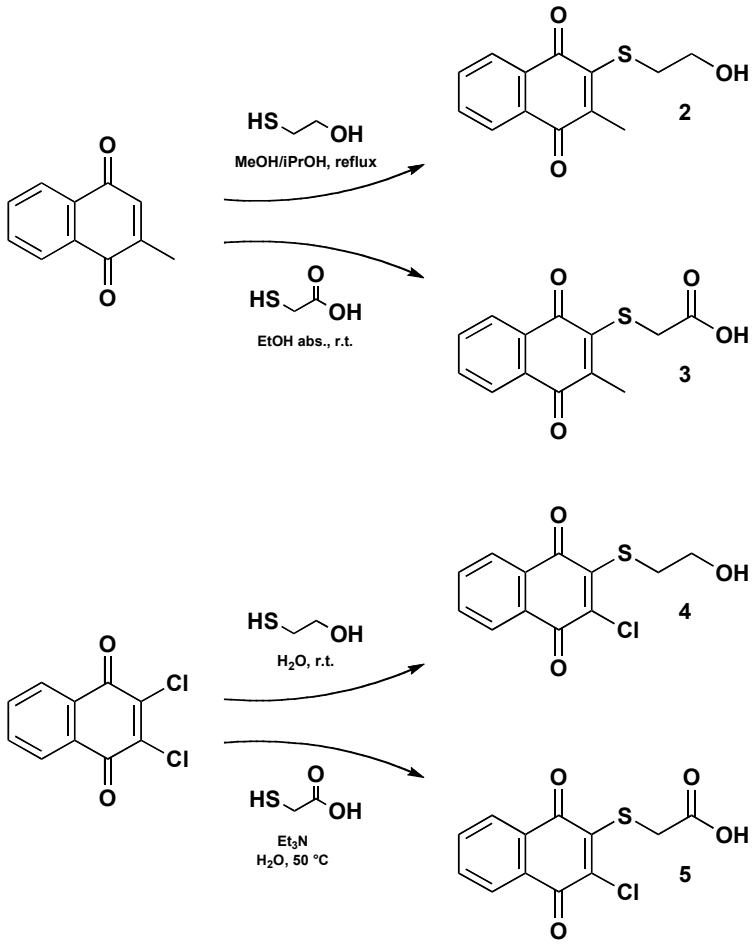

Figure 18: General procedure for the synthesis of *O,S*-chelating naphthoquinone based ligands

Ligands **2**[88], **3**[91], **4** and **5**[92] were synthesized according to literature procedures in good to excellent yields (57–90%) (see Figure 18). Purification of ligand **2** (known as Cpd 5 in literature), however, was performed *via* flash column chromatography, and no extraction

[91] Tandon, V.K., Yadav, D.B., Singh, R.V., Vaish, M., Chaturvedi, A.K., and Shukla, P.K., *Bioorganic & Medicinal Chemistry Letters*, **2005**, 15, 3463-66.
[92] Tandon, V.K., Maurya, H.K., Verma, M.K., Kumar, R., and Shukla, P.K., *Eur. J. Med. Chem.*, **2010**, 45, 2418-26.

and/or washing procedures were preceded as described in literature. A higher yield (69% instead of 40%) could be achieved by this modification. The acetic acid residue in both compounds **3** and **5** provides advantages for the purification process, which was done *via* extraction. Both compounds **4** and **5** were synthesized on water based "green chemistry" deriving from 2,3-dichloro-1,4-naphthoquinone, and no purification was needed for ligand **4**, which resulted in high yields. The obtained ligands were characterized by 1D NMR and elemental analysis.

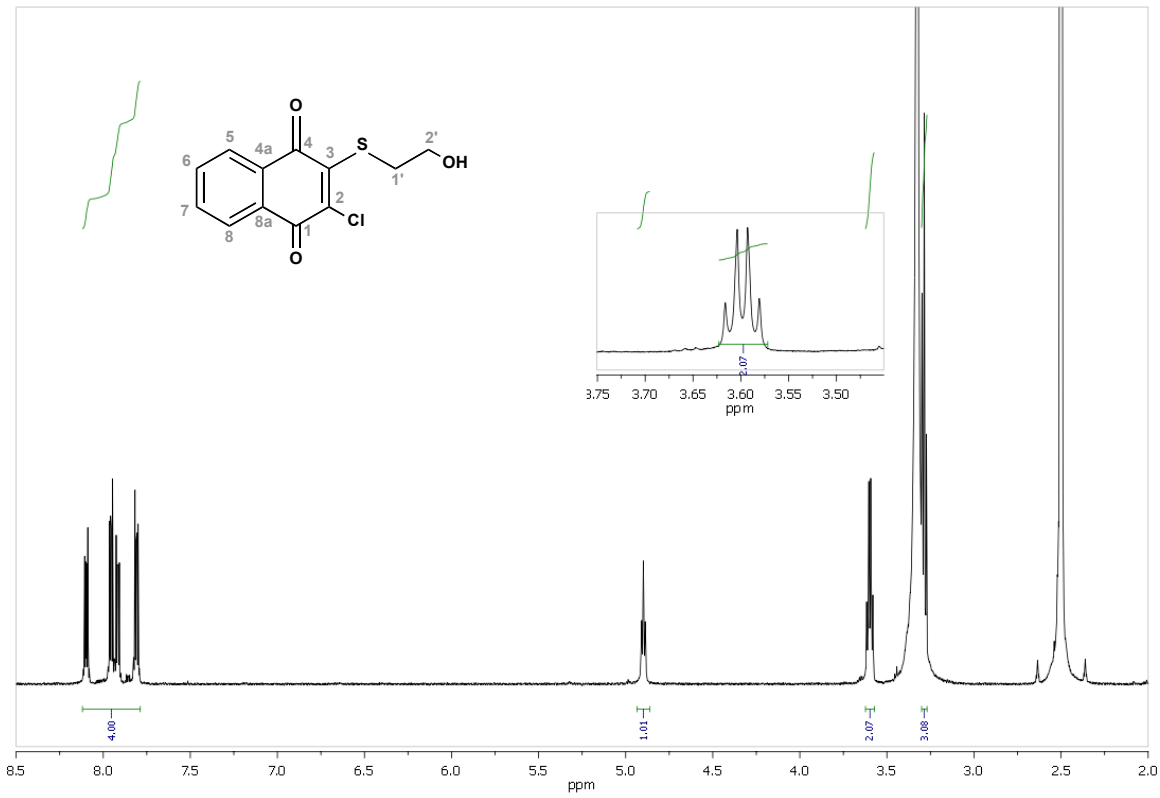

Figure 19: ^{1}H – NMR of ligand 4

Figure 19 shows the ^{1}H-NMR of ligand **4**. The peak at 3.60 was assigned to the two hydrogen atoms at position 2'. These two hydrogens couple with the CH_2 group at position 1' and with the hydrogen of the hydroxy group, and give therefore a doublet of triplets with equal coupling constant values resulting in a quartet with 1:3:3:1 intensity. The same applies to the ^{1}H-NMR of ligand **2**.

2.1.2 COMPLEXATION APPROACHES

One part of the thesis was the coordination of *O,S*-chelating ligands to an organometallic fragment to obtain positively charged complexes with increased water solubility, which was further augmented by the additional hydroxy rest in ligands **2** and **4**. Classical complexation synthesis was not successful for the synthesis of the complexes of ligands **2**-**5**. Various approaches were tried, but ligands **2** and **4** were not able to coordinate to the metal center *via* the oxygen of the carbonyl from the naphthoquinone and the sulfur to form a five-membered ring. Various approaches were tried to synthesize the complexes: different solvents were used ((dry)MeOH, (dry)EtOH, (dry)DCM, toluol), variation in the reagent ratio (small excess of the ligand, 1:1 ratio dimer and ligand), temperature (room temperature, refluxing temperature of the respective solvent), different bases (NaOMe, Et_3N, NaOH, NMM), microwave approaches. NMRs were recorded after 1-24 hours. Complexation was observed for ligands **3** and **5** only, whereby ligand **5** showed better results and was investigated synthetically further. The best synthetic approach occurred in methanol *via* the use triethylamine, and by refluxing the reaction mixture (Figure 20 shows the ^{1}H-NMR of complex **5a)**. The two hydrogen atoms at position 1' are now splitted due to the formation of an inflexible ring, leading to the statement that coordination takes place. However, it is remarkable that there are two complex species formed, with an intensity of 1:2, see aromatic hydrogen signals of the cymene moiety in the range between 6.2 and 5.7 ppm, or CH_3 signals at around 2.3 and 2.2 ppm.

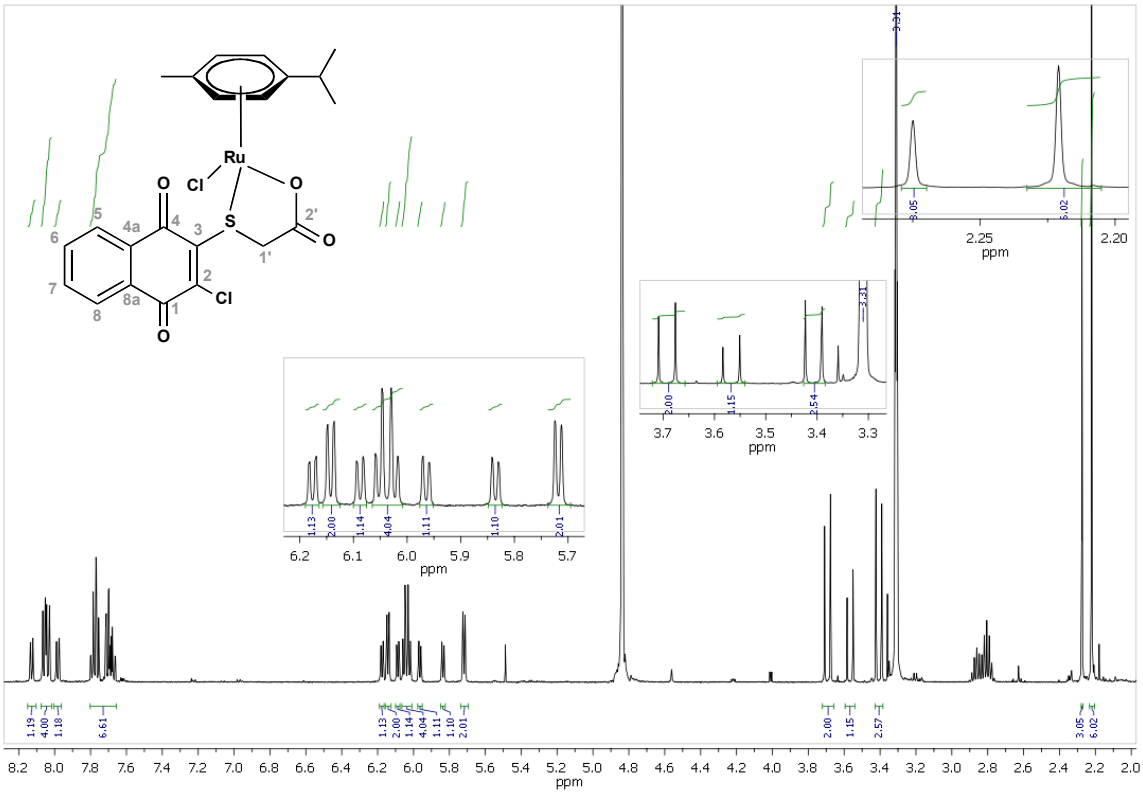

Figure 20: ^{1}H – NMR of complex 5a

2.1.3 SEPARATION APPROACHES

It was possible to separate the two compounds on the analytical HPLC, however, separation on preparative HPLC was not possible. ESI-MS measurements were made to identify the peaks, but for both, one and the same peak was observed, which remains not identifiable.

2.2 ORGANOMETALLIC ANTICANCER COMPLEXES OF LAPACHOL: METAL CENTRE-DEPENDENT FORMATION OF REACTIVE OXYGEN SPECIES AND CORRELATION WITH CYTOTOXICITY

Multi-targeted drugs are a hot topic of research in cancer chemotherapy, because this approach provides a remedy of overcoming disadvantages and limitations of currently used drugs. With the use of more than one pharmacophore, a redox active ligand system and a bioactive metal center, it is tried to improve anticancer activity. The aim of the work was the synthesis of ruthenium-, osmium- and rhodium- coordinated lapachol complexes. Lapachol is ascribed to have antibiotic and anticancer properties and was investigated in clinical trials as an anticancer agent. The obtained organometallic complexes were characterized by 1D and 2D NMR spectroscopy, melting point and elemental analysis. It was possible to obtain the crystal structures of ruthenium and rhodium complexes by X-ray diffraction analysis. Furthermore, their stability was examined *via* UV/Vis spectroscopy and ESI-MS measurements, and the interaction with amino acids and proteins was investigated by ESI-MS. These studies were accompanied by *in vitro* experiments to elucidate their anticancer potential and their biological target. The *in vitro* anticancer activity of the synthesized complexes was determined by the colorimetric MTT assay in different human tumor cell lines, and moreover the generation of reactive oxygen species and the influence on the cell cycle were investigated. These experiments showed that the compounds are cytotoxic in the low µM range and that they induce apoptosis by a mode of action involving oxidative stress; this effect was especially pronounced in case of the organoruthenium compound.

2.2.1 SYNTHESIS OF THE LAPACHOL COMPLEXES

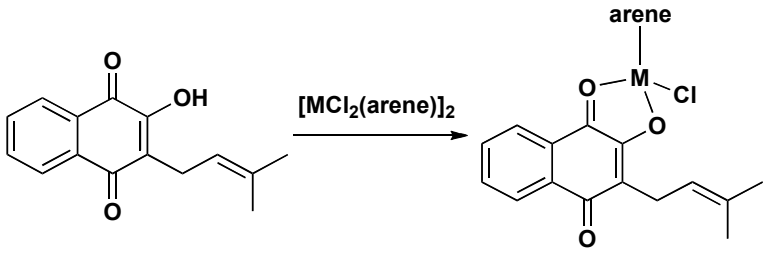

L **1a-c**

Figure 21: Synthetic pathway to the lapachol complexes 1a–c (M = Ru^{II}, Os^{II}, Rh^{III}; arene = η^6-*p*-cymene for Ru^{II}, Os^{II} and η^5-pentamethylcyclopentadiene for Rh^{III}).

General procedure of the products consists in the complexation of lapachol with the corresponding dimeric metal precursor (Figure 21). The ligand was used in a slight excess to facilitate purification. The organometallic complexes **1a-c** were synthesized by deprotonating commercially available lapachol **L** with sodium methoxide followed by conversion with the respective dimer $[MCl_2(arene)]_2$ (M = Ru^{II} **1a**, Os^{II} **1b**, Rh^{III} **1c**; arene = η^6-*p*-cymene for Ru^{II}, Os^{II} and η^5-pentamethylcyclopentadiene for Rh^{III}) to the corresponding organometallics **1a-c** in good to excellent yields (75–96%).

2.2.2 CRYSTALLOGRAPHIC STRUCTURE DETERMINATION

Single crystals of **1a** and **1b** suitable for X-ray diffraction analysis (Table 2) were obtained from dichloromethane/*n*-hexane by using the slow diffusion method. Complexes **1a** and **1b** crystallize in the monoclinic space group P21/n and adopt the pseudo-octahedral “piano-stool” configuration (Figure 22), which is typical for this class of organometallic compounds. Lapachol acts as an anionic bidentate *O,O*-chelating ligand leading to the formation of a five-membered, non-planar (torsion angle O1-M-O2-C1 is in both cases unequal zero) ring with envelope conformation. The M–O2 distances were slightly shorter (2.0764(10) Å for **1a**, 2.077(2) Å for **1b**) than the corresponding M–O1 bond lengths (2.1072(11) Å for **1a**, 2.128(2) Å for **1b**), which is in good agreement with data obtained for related organometallic complexes.

The coordination of the keto group to the metal center induces an elongation of the C–O bond length of the coordinated carbonyl group (1.259(4) Å for **1b**) as compared to the uncoordinated carbonyl in *para*-position (1.240(4) Å for **1b**), which confirms the 1,4-dioxo form of the attached ligand. Compared to the usual carbonyl bond length of 1.20 Å, both carbonyl bond lengths in the complexes **1a** and **1b** are longer, because of

the electron withdrawing effect of the transition metal center.

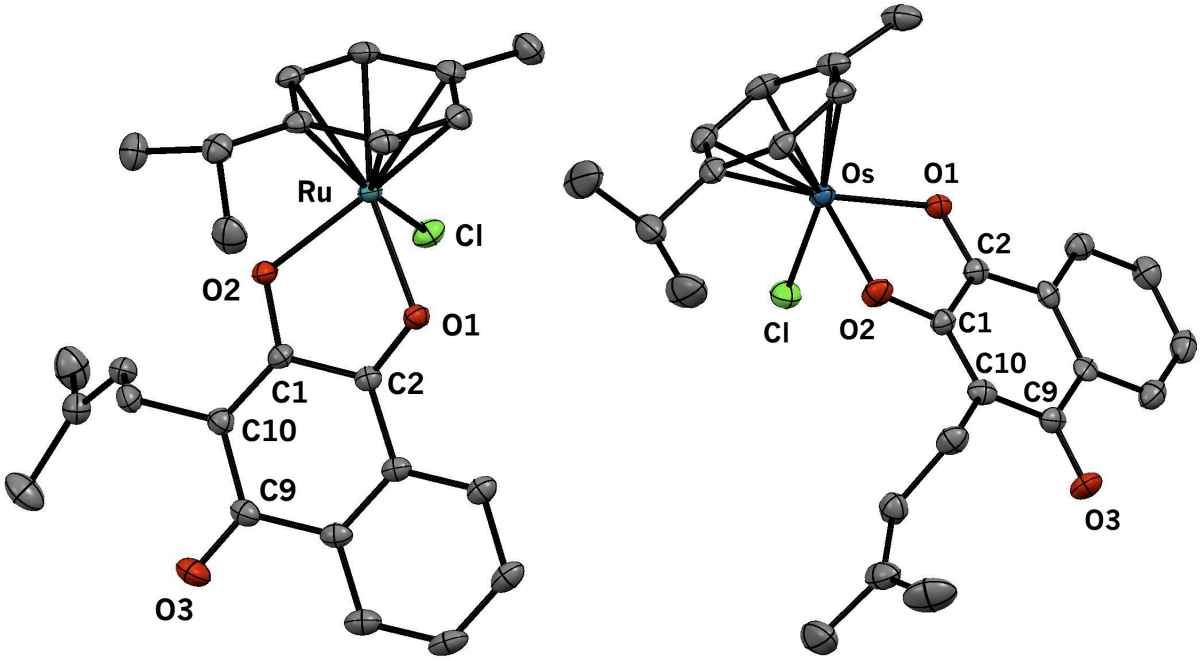

Figure 22: Molecular structure of the $M^{II}(\eta^6$-*p*-cymene) complexes 1a (M = Ru; left) and 1b (M = Os; right) drawn at 50% probability level. The hydrogen atoms were omitted for clarity.

Table 1: Relevant bond lengths and angles

Compound	1a	1b
M-O1 [Å]	2.1072(11)	2.128(2)
M-O2 [Å]	2.0764(10)	2.077(2)
M-Cl [Å]	2.4065(4)	2.3886(9)
C1-O2 [Å]	1.3031(17)	1.304(4)
C2=O1 [Å]	1.2470(17)	1.259(4)
C1-C2 [Å]	1.475(2)	1.470(4)
C9=O3 [Å]	1.2289(19)	1.240(4)
O2-M-O1 [°]	77.15(4)	75.70(9)
O2-M-Cl [°]	86.22(3)	84.99(7)
O1-M-Cl [°]	82.33(3)	82.37(6)
C2=O1-M [°]	114.32(9)	114.8(2)
C1-O2-M [°]	114.77(9)	115.78(19)
O2-C1-C2 [°]	115.18(12)	114.8(3)
O1=C2-C1 [°]	117.54(13)	116.5(3)
O3=C9-C10 [°]	121.64(15)	121.2(3)
O1-M-O2-C1 [°]	-6.92(10)	-12.9(2)

Table 2: Crystal data and details of data collection for 1a and 1b

	1a	1b
Chemical formula	$C_{25}H_{27}ClO_3Ru$	$C_{25}H_{27}ClO_3Os$
M (g mol^{-1})	511.99	601.12
Temperature (K)	150(2)	150(2)
Crystal size (mm)	0.60 × 0.10 × 0.10	0.12 × 0.10 × 0.02
Crystal color, shape	blue, block	violet, block
Crystal system	monoclinic	monoclinic
Space group	$P2_1/n$	$P2_1/n$
a (Å)	12.8956(5)	13.4764(4)
b (Å)	11.8913(4)	8.4120(2)
c (Å)	14.2756(5)	21.0225(5)
α (°)	90	90
β (°)	98.501	107.9860
γ (°)	90	90
V (Å^3)	2165.05(13)	2266.72(10)
Z	4	4
D_c (g cm^{-3})	1.571	1.761
μ (mm^{-1})	0.872	5.767
F (000)	1048	1176
θ range (°)	1.99 – 30.07	2.14 – 28.00
h range	-18/18	-17/17
k range	-16/16	-9/11
l range	-20/17	-27/27
no. reflections	50326	17682
no. parameters	274	274
R_{int}	0.0382	0.0426
R_1[a]	0.0225	0.0247
wR_2[b]	0.0595	0.0507
GOF[c]	1.000	0.997
Residuals (e$^-$ Å^{-3})	0.645, -0.394	0.806, -0.648

[a] $R_1 = \Sigma||F_o| - |F_c||/\Sigma w|F_o|$, [b] $wR_2 = \{\Sigma[w(F_o^2 - F_c^2)^2]/\Sigma[w(F_o^2)^2]\}^{1/2}$, [c] $S = \{\Sigma[w(F_o^2 - F_c^2)^2] / (n - p)\}]^{1/2}$,where n is the number of reflections and p is the total number of parameters refined.

2.2.3 UV/VIS SPECTROSCOPY

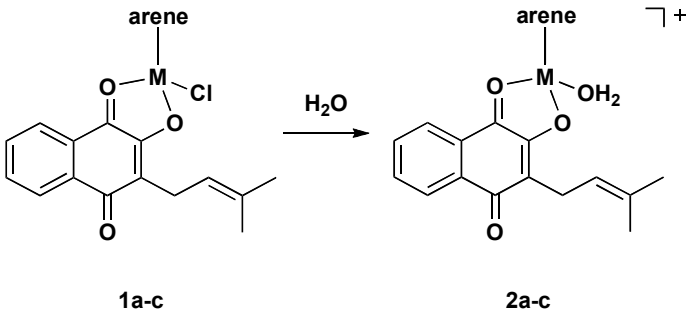

Figure 23: Structural representation of aqueous solution behavior of the complexes

The behavior in aqueous solution of the organometallic lapachol complexes with respect to the aquation was studied at 298 K by UV/Vis spectroscopy. Figure 24 depicts the UV/Vis spectra of the Ru-, Os- and Rh- complexes of lapachol (**1a**, **1b** and **1c** respectively) in 1% DMSO/PBS. The strong absorbance maxima in between 220 and 300 nm can be attributed to intraligand π-π* transitions. A further absorption is seen at 480, 490, 350 nm respectively, which can presumably be attributed to metal-to-ligand charge transfer. All complexes undergo hydrolysis and are readily conversed to the corresponding aqua species, but are then quite stable in aqueous solution for a significant time.

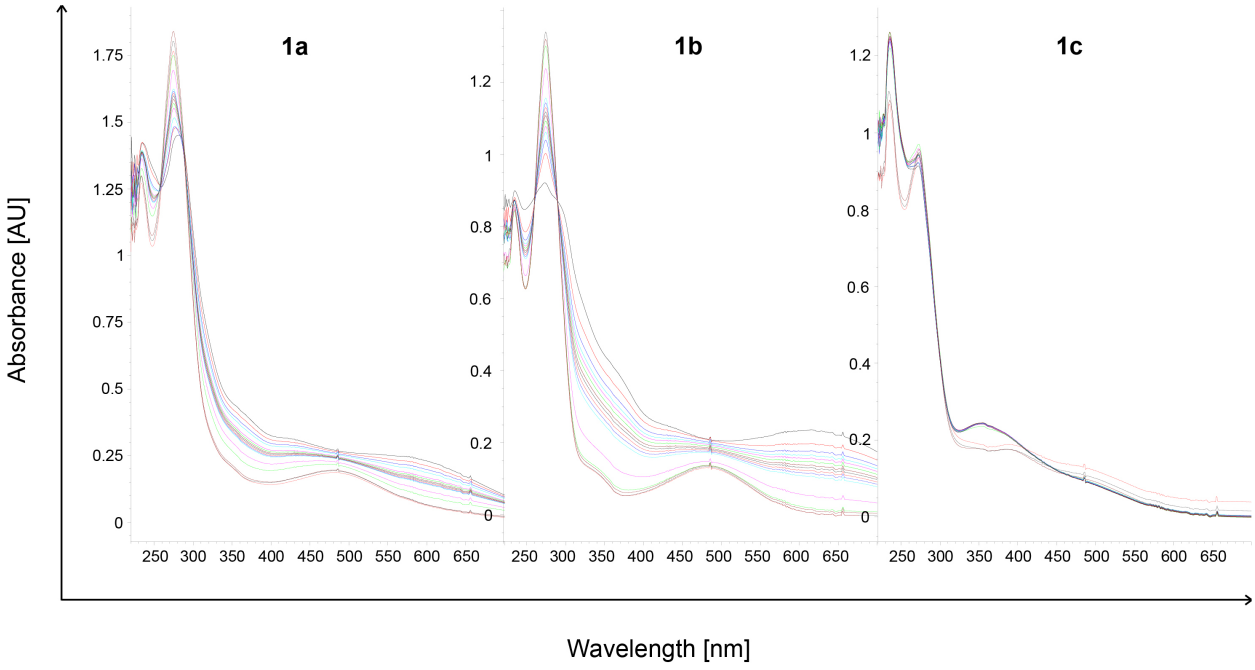

Figure 24: UV/Vis spectra of complexes 1a-c in 1% DMSO/PBS

2.2.4 ESI-MS STABILITY AND BIOMOLECULE INTERACTION STUDIES

To further investigate the nature of changes observed in UV/Vis spectra, the aqueous chemistry of the lapachol-containing organometallics **1a–c** was studied by ESI-IT-MS (Figure 23). In all cases, the formation of M(arene) dimers was observed accompanied by ligand release and resulted in the formation of chlorido-bridged (**2c**) and hydroxido-bridged (**2a**, **2b**) dimers. The extent of ligand release followed the order **2c** < **2a** < **2b**, *i.e.* compound **2c** is largely stable for at least 24 h, while ligand release was virtually quantitative for **2b** (see Figure 25).

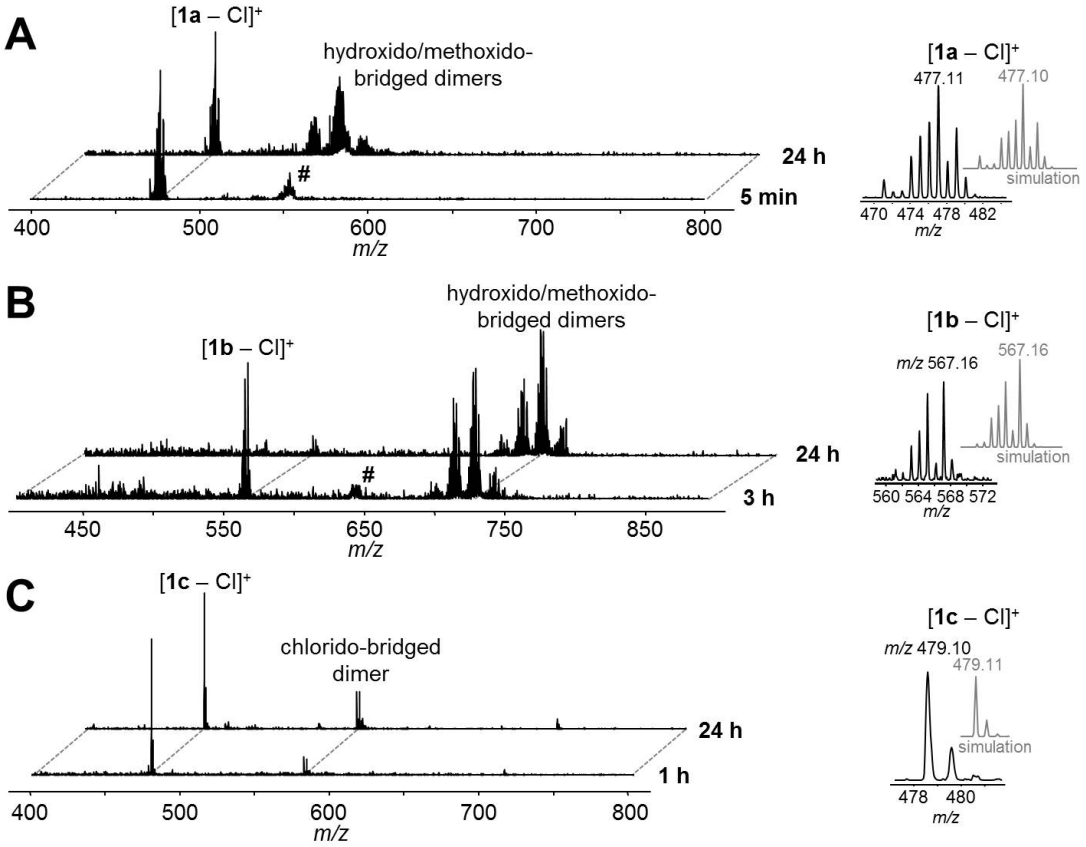

Figure 25: The stability of 1a (A), 1b (B) and 1c (C) in water was determined by ESI-IT-MS and representative mass spectra are shown. The different types of dincuclear species in A and B stem from the dilution with H_2O : MeOH (1 : 1) prior to infusion into the mass spectrometer and correspond to $[(cym)M(\mu\text{-}OH)_{n\text{-}3}(\mu\text{-}OCH_3)_n]^+$, where M is Ru (n = 1 – 3) or Os (n = 0 – 3). DMSO adducts of the general formula $[1a,b – Cl + DMSO]^+$ were only detected in small amounts during the first hours of incubation and the signals are annotated with #.

Table 3 Experimental and theoretical *m/z* vlaues of the observed metal-containing species in incubation mixtures of 1a–c in aqueous solution and in the presence of biological nucleophiles. The measured *m/z* values on the ESI-IT-MS include a standard deviation of *m/z* ± 0.05.

	Detected Ion	*m/z*	m_{theor}
ESI-IT-MS	[**1a** – Cl]$^+$	477.11	477.10
	[(cym)$_2$Ru$_2$(μ-OH)$_2$(μ-OCH$_3$)]$^+$	537.04	537.05
	[(cym)$_2$Ru$_2$(μ-OH)(μ-OCH$_3$)$_2$]$^+$	551.04	551.07
	[(cym)$_2$Ru$_2$(μ-OCH$_3$)$_3$]$^+$	565.06	565.08
	[(cym)Ru(Met) – H$^+$]$^+$	386.06	396.06
	[(cym)Ru(His) – H$^+$]$^+$	390.07	390.08
	[(cym)Ru(L)(EtG)]$^+$	656.17	656.18
	[**1b** – Cl]$^+$	567.16	567.16
	[(cym)$_2$Os$_2$(μ-OH)$_3$]$^+$	701.12	701.15
	[(cym)$_2$Os$_2$(μ-OH)$_2$(μ-OCH$_3$)]$^+$	715.11	715.16
	[(cym)$_2$Os$_2$(μ-OH)(μ-OCH$_3$)$_2$]$^+$	729.15	729.18
	[(cym)$_2$Os$_2$(μ-OCH$_3$)$_3$]$^+$	743.19	743.19
	[(cym)Os(Cys) – H$^+$]$^+$	446.04	446.08
	[(cym)Os(Met) – H$^+$]$^+$	474.10	474.11
	[(cym)Os(His) – H$^+$]$^+$	480.11	480.13
	[(cym)Os(L)(EtG)]$^+$	746.21	746.24
	[**1c** – Cl]$^+$	479.10	479.11
	[(Cp*)$_2$Rh$_2$(μ-Cl)$_3$]$^+$	580.93	580.95
	[(Cp*)Rh(Met) – H$^+$]$^+$	386.05	386.07
	[(Cp*)Rh(His) – H$^+$]$^+$	392.07	392.08
	[(Cp*)Rh(L)(Cys)]$^+$	600.11	600.13
	[(Cp*)Rh(L)(Met)]$^+$	628.14	628.16
	[(Cp*)Rh(L)(His)]$^+$	634.15	634.18

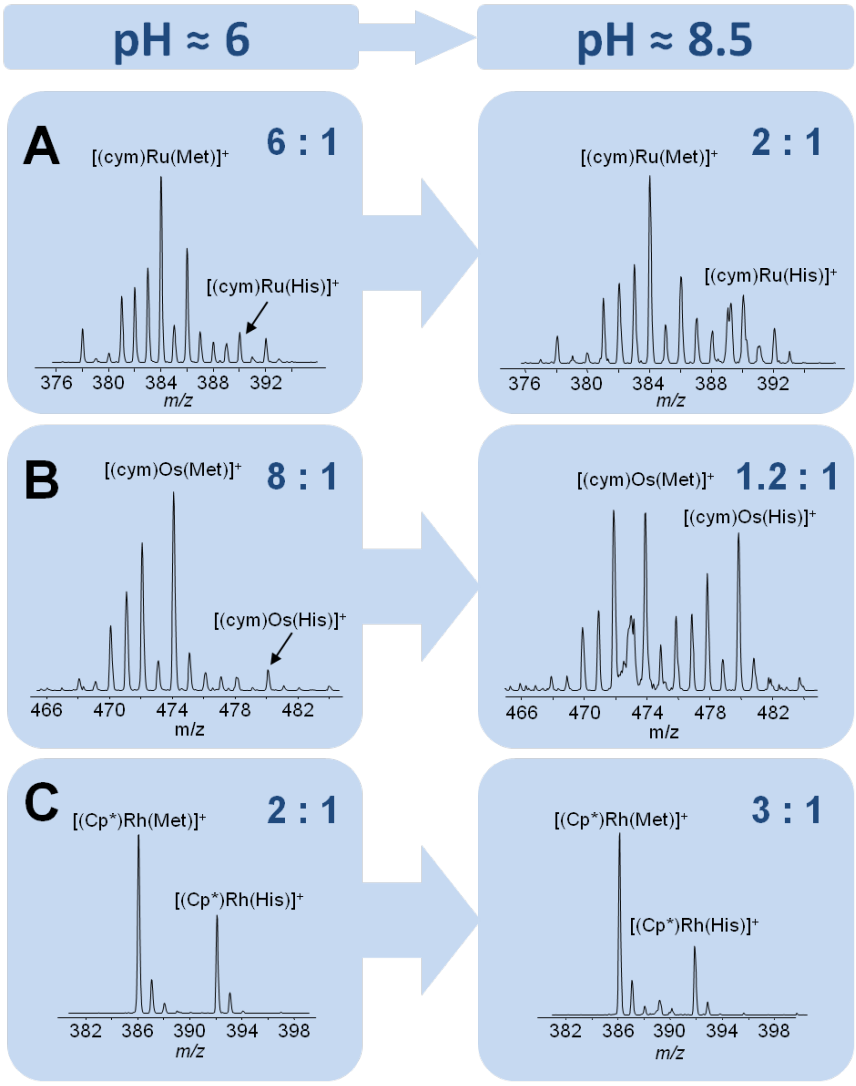

Figure 26: pH-Dependent adduct formation of 1a (A), 1b (B) and 1c (C) with Met and His. The ratio between the abundance of the Met and the His adducts is given.

The reactivity of metal complexes towards biomolecules is a crucial parameter for their biological activity. Therefore, **1a–c** were exposed to a mixture containing the DNA model 9-ethylguanine (EtG) and the amino acids glycine (Gly), L-cysteine (Cys), L-histidine (His) and L-methionine (Met). EtG adducts were only transiently formed during the first hour and were only observed for **1a** and **1b**, while Gly adducts were not detected. Compounds **1a–c** displayed similar thermodynamically stable products, corresponding to His and mainly Met adducts detected as $[M(aa) - H]^+$ ions (M = (Cp*)Rh, (cym)Ru or (cym)Os; aa = His or Met). Interestingly, different reaction pathways were observed for **1a–c**. **1c** transiently formed Cys adducts, which disappeared again after 24 h. A two-step binding process of amino acids was detected involving initial mono-dentate coordination of an amino acid which induces the labialization of the *O,O*-chelate and leads ultimately to cleavage of lapachol. In contrast

to **1c**, **1a** directly formed His and Met adducts and no other adducts were detected. For **1b**, Cys adducts are stable for more than 24 h were observed besides His and Met adducts (Table 3). The extent of His or Met adduct formation seems to be pH dependent (Figure 26), which is of relevance in certain slightly more acidic solid tumors due to hypoxia or upregulated glycolysis.[30] In such an environment, the organometallic Rh^{III}, Ru^{II} and Os^{II} compounds seem to favor thioether over imine binding. In addition, the reactivity of **1a–c** toward the model protein ubiquitin (ub) was investigated using ESI-TOF-MS. Incubation of **1a–c** with ub (2 : 1) for 24 h yielded primarily monoadducts accompanied by lapachol release ligand from the metal center (Figure 27; Table 4). These monoadducts were then subjected to in-source collision-induced dissociation (ISCID), in order to obtain information on the binding site of the metal ion on the protein. Detection of $^{Ru(cym)}A_1$ and $^{Os(cym)}B_1$ fragments suggest Met1 as the primary binding site for **2a** and **2b**, as did the fragment $^{(Cp^*)Rh}B_3$ for **2c** (Table 5). To the best of our knowledge, this is the first report on binding site determination of a Rh-metallodrug on a protein in a top-down approach.

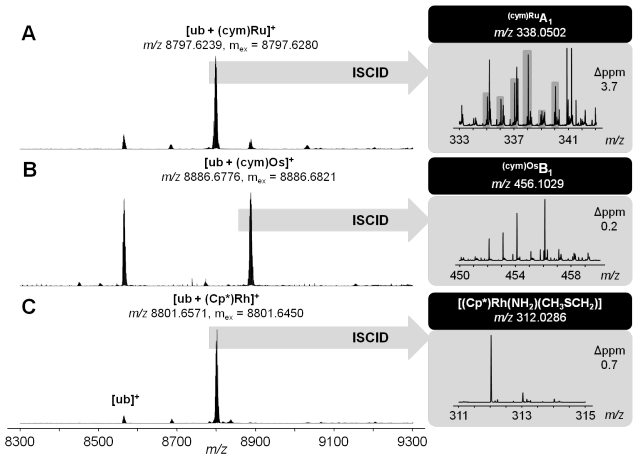

Figure 27: Ultra-high resolution ESI-TOF mass spectra of 2 : 1 reaction mixtures containing 1a (A), 1b (B) or 1c (C) and after 24 h (left) ISCID top-down signals of the respective mono-adduct reveal Met1 as the primary metallation site (right).

Table 4: Accurate and exact masses of the metal-containing species obtained by incubation of 1a–c with ubiquitin (ub). The accuracy of the ESI-TOF-MS measurements is given in Δppm.

	Deconvoluted Ion	m_{acc}	m_{ex}	Δppm
ESI-TOF-MS	ub^+	8564.6255	8564.6299	0.5
	$[ub + (Cp^*)Rh]^+$	8801.6571	8801.6450	1.4
	$[ub + Ru(OH)]^+$	8683.5649	8683.5444	2.4
	$[ub + (cym)Ru]^+$	8797.6239	8797.6280	0.5
	$[ub + 2(cym)Ru]^+$	9031.6104	9031.6282	2.0
	$[ub + (cym)Os]^+$	8886.6776	8886.6821	0.5

Table 5: Metallated peptide fragments obtained by top-down mass spectrometry of mono-adduct formed from the reaction between 1a–c and ubiquitin using ISCID fragmentation on the ESI-TOF-MS. The relative abundance (%) refers to the most abundant mass signal in the ISCID spectrum.

Fragment	z	m_{acc}	m_{ex}	Δppm	%
[ub + (cym)Ru]					
$^{(cym)Ru}A_1$	1	338.0502	338.0514	3.7	6.8
$^{(cym)Ru}B_7$	2	541.7401	541.7384	3.3	8.1
$^{(cym)Ru}B_{13}$	3	565.9543	565.9549	1.1	6.7
$^{(cym)Ru}A_{14}$	3	590.3070	590.3059	1.9	14.7
$^{(cym)Ru}A_{15}$	3	627.9995	628.0006	1.8	12.2
$^{(cym)Ru}B_{16}$	3	680.3498	680.3465	4.9	42.8
$^{(cym)Ru}B_{18}$	3	756.3869	756.3836	4.3	18
[ub + (cym)Os]					
$^{(cym)Os}B_1$	1	456.1029	456.1030	0.2	11.8
$^{(cym)Os}B_2$	1	584.1602	584.1616	2.3	3.8
$^{(cym)Os}A_{13}$	3	586.6448	586.6419	5.1	4.0
$^{(cym)Os}B_{14}$	3	629.6585	629.6561	3.9	6.8
$^{(cym)Os}B_{18}$	3	786.4048	786.4021	3.4	6.4
[ub + (Cp*)Rh]					
(Cp*)Rh($^{\cdot}CH_2SCH_3$)(NH_2)	1	312.0286	312.0288	0.7	42.5
$^{(Cp^*)Rh}B_3$	1	609.1981	609.1976	0.8	3.7
$^{(Cp^*)Rh}A_7$	3	352.8323	352.8323	0.2	1.4
$^{(Cp^*)Rh}B_{12}$	3	528.9297	528.9292	0.9	12.5
$^{(Cp^*)Rh}A_{13}$	3	557.2945	557.2922	4.0	16.8
$^{(Cp^*)Rh}A_{14}$	3	590.9767	590.9748	3.2	15.2
$^{(Cp^*)Rh}B_{15}$	3	638.3350	638.3354	0.8	20.1
$^{(Cp^*)Rh}A_{16}$	3	672.0169	672.0180	1.6	9.9
$^{(Cp^*)Rh}B_{16}$	3	681.3501	681.3496	0.6	47.3
$^{(Cp^*)Rh}B_{18}$	3	757.3824	757.3866	5.5	14

2.2.5 CYTOTOXICITY IN CANCER CELL LINES

The cytotoxicity of the organometallic complexes **1a–c** was determined by the colorimetric MTT assay in the human cancer cell lines CH1 (ovarian carcinoma), SW480 (colon carcinoma) and A549 (non-small cell lung carcinoma) and was compared to lapachol and cisplatin (Table 6 and Figure 28). Complexes **1a–c** exhibit antitumor activity in the low μM range. In general, the activity of **1b** was widely similar to that of lapachol (**L**), indicating that the ligand was the cytotoxicity-determining moiety of the compound. This may be related to ligand release in the presence of biomolecules as shown by the MS studies. The rhodium complex **1c** was less cytotoxic than lapachol and more stable under physiological conditions. The organoruthenium compound **1a** was the most potent compound of the series, which might be explained by a synergistic effect of metal ion coordination.

Table 6: *In vitro* anticancer activity[a] (IC_{50} values in μM) of 1a-c in CH1, SW480 and A549 cells compared to cisplatin and lapachol (L).[a]

	CH1	SW480	A549
L	3.3 ± 0.2	5.5 ± 0.6	42 ± 14
1a	4.1 ± 0.6	4.1 ± 1.5	20 ± 5
1b	4.2 ± 0.8	9.0 ± 1.1	46 ± 8
1c	7.3 ± 1.5	39 ± 12	91 ± 19
cisplatin	0.14 ± 0.03[b]	3.3 ± 0.4[b]	1.3 ± 0.4[b]

[a] 96 h exposure; [b] taken from ref.[93]

MTT results for the A549 cell line show a flat curve shape, and therefore a standard deviation, which in some cases exceeds 30% deviation, is still accepted.

[93] Scaffidi-Domianello, Y.Y., Legin, A.A., Jakupec, M.A., Arion, V.B., Kukushkin, V.Y., Galanski, M., and Keppler, B.K., *Inorganic Chemistry*, **2011**, 50, 10673-81.

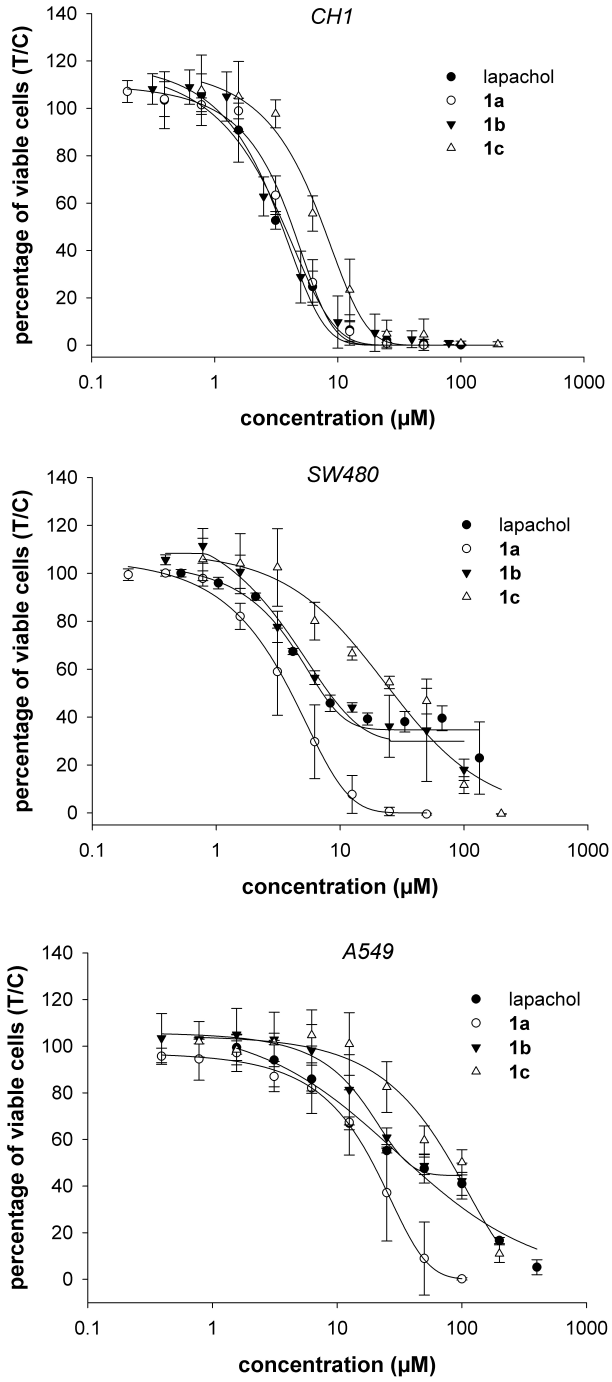

Figure 28: Concentration-effect curves determined for lapachol and its Ru, Os and Rh complexes in the human tumor cell lines CH1, SW480 and A549.

2.2.6 INVESTIGATION OF REACTIVE OXYGEN SPECIES GENERATION

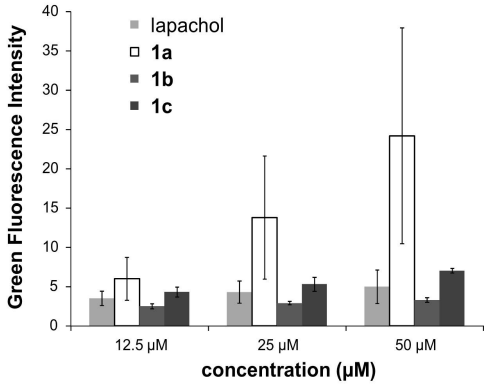

Figure 29: Determination of the ROS level induced by lapachol and 1a-c by the DCFH-DA-assay.

The cytotoxic activity of lapachol is related to the generation of ROS and interaction with nucleic acids.[82,94] Thus the potential of **1a–c** to induce oxidative stress through ROS was investigated by means of the DCFH-DA assay in HL60 (promyelocytic leukemia, human) cells. **1a** was found to generate ROS to a higher extent than the free ligand and the osmium and rhodium compounds (Figure 29). This observation confirms a synergistic effect of the organoruthenium coordination to the bioactive quinone.

[94] Hillard, E.A., de Abreu, F.C., Ferreira, D.C.M., Jaouen, G., Goulart, M.O.F., and Amatore, C., *Chemical Communications*, **2008**, 0, 2612-28.

2.2.7 CELL CYCLE ANALYSIS

In addition, the impact of **L** and **1a–c** on the cell cycle was investigated by FACS analysis in CH1 cells. Treatment of CH1 cells with the corresponding compound at the concentration of the respective IC_{50} range and lower caused a substantial arrest in the S phase (Figure 30).

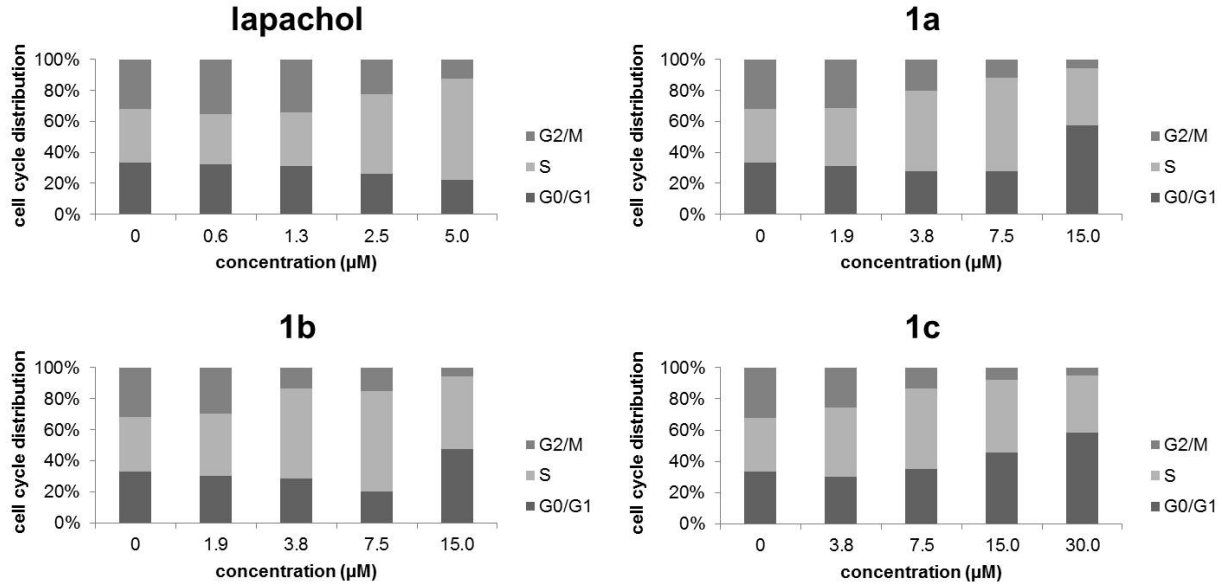

Figure 30: Concentration-dependent impact of lapachol and its Ru, Os and Rh complexes on the cell cycle distribution of CH1 after exposure for 24 h (values are means of three independent experiments).

3 EXPERIMENTAL PART

3.1 EQUIPMENT, MATERIALS AND METHODS

Chemicals

Menadione and triethylamine were purchased from Fisher, 2-mercaptoethanol (purity about 99%) and 2,3-dichloronaphthoquinone from Sigma Aldrich, and thioglycolic acid (purity about 80%) from Merck.

Absolute methanol was dried according to standard procedures. Lapachol, sodium methoxide and pentamethylcyclopentadiene were purchased from Sigma Aldrich, α-terpinene from Acros Fischer, rutheniumtrichloride trihydrate from Degussa, osmiumtetroxide and rhodiumtrichloride hydrate from Johnson Matthey, hydrazine dihydrochloride from Fluka, and hydrochloric acid from Merck. All these chemicals were used without further purification.

The ruthenium- and osmium-arene starting compounds $[M(\eta^6\text{-}p\text{-cymene})(Cl)(\mu\text{-}Cl)]_2$($M = Ru^{II}$, Os^{II}) and the rhodium-arene dimer $[Rh(Cp^*)(Cl)(\mu\text{-}Cl)]_2$ were prepared as described in literature.[95,96,97] For the preparation of $[Os(p\text{-cymene})(Cl)(\mu\text{-}Cl)]_2$, OsO_4 was reduced by $N_2H_4 \cdot 2\,HCl$ in concentrated HCl to $H_2[OsCl_6]$, and then reacted with α-terpinene.

Equipment

^1H-, $^{13}C\{^1H\}$- and two-dimensional NMR spectra were recorded at 298 K on a Bruker Avance III™ 500 MHz spectrometer at 500.10 (^1H) and 125.75 MHz (^{13}C). Elemental analyses were performed by the Microanalytical Laboratory of the Faculty of Chemistry of the University of Vienna, on a Perkin Elmer 2400 CHN elemental analyzer. Electrospray ionization mass spectrometry (ESI-MS) was carried out with a Bruker Esquire 3000 instrument (Bruker Daltonics, Bremen, Germany).

X-ray diffraction analyses of **1a** and **1b** were performed on a Bruker X8 APEX II CCD diffractometer at 150 K. Single crystals were positioned at 40 mm from the detector and 1144 frames for 5 s exposure time over 1° scan width were measured for **1a**, and 449 frames for 60 s over 1° scan for **1b**.

Melting points were determined by the use of a Büchi Melting Point M-560.

---

[95] Bennett, M.A. and Smith, A.K., *J. Chem. Soc., Dalton Trans.*, **1974**, 233-41.
[96] Kiel, W.A., Ball, R.G., and Graham, W.A.G., *J. Organomet. Chem.*, **1990**, 383, 481-96.
[97] Booth, B.L., Haszeldine, R.N., and Hill, M.P., *J. Chem. Soc. A*, **1969**, 1299-303.

The solubility was determined by dissolving the compound in DMSO and dropwise diluting with PBS to get a final concentration of 1% DMSO/PBS. The highest concentrated dilution, where no precipitation of the compound occurred, was the determined solubility.

3.2 *O,S*-CHELATES

3.2.1 SYNTHESIS OF THE LIGANDS

3.2.1.1 2-(2-Hydroxy-ethylthio)-3-methyl-1,4-naphthoquinone (2)

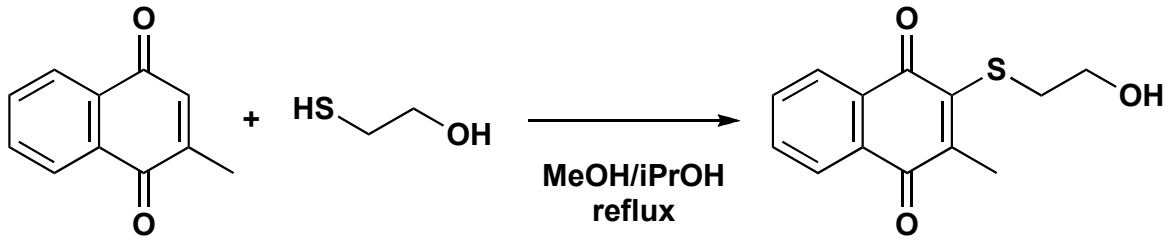

[172.18] [78.13] [248.30]

Synthesis

Menadione (100 mg, 0.58 mmol, 1 eq) was dissolved in a mixture of methanol (10 mL) and 2-propanol (8 mL). 2-Mercaptoethanol (150 µL, 2.14 mmol, 3.7 eq) was added and the solution was refluxed for 24 hours. The solvent was evaporated and the crude product, a brown oil, was dried *in vacuo*.
Purification was performed *via* flash column chromatography (*n*-hexane / ethyl acetate, 5:1).

Yield 99 mg (69%), yellow solid

Elemental analysis for $C_{13}H_{12}O_3S$

	C [%]	H [%]	O [%]	S [%]
calculated	62.88	4.87	19.33	12.91
found	62.41	4.91	19.49	12.68
Δ	0.47	-0.04	-0.16	0.23

NMR-spectroscopy

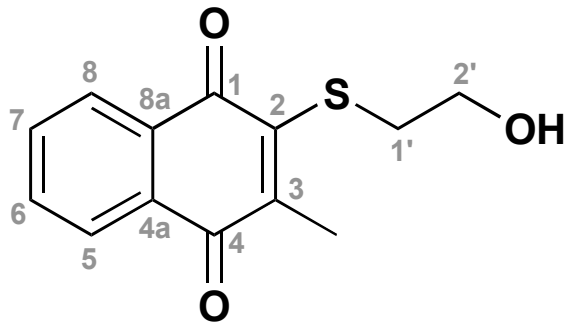

^{1}H NMR (500.10 MHz, DMSO-d_6) δ: 8.01 – 7.97 (m, 2H, H-6, H-7), 7.86 – 7.79 (m, 2H, H-5, H-8), 4.86 (t, ^3J(H,H) = 5 Hz, 1H, OH), 3.59 (dt, ^3J(H,H) = 6 Hz, ^3J(H,H) = 6 Hz, 2H, H-2'), 3.25 (t, ^3J(H,H) = 6 Hz, 2H, H-1'), 2.26 (s, 3H, CH_3).

3.2.1.2 2-(3-Methyl-1,4-dioxo-1,4-dihydronaphthalen-2-ylthio)acetic acid (3)

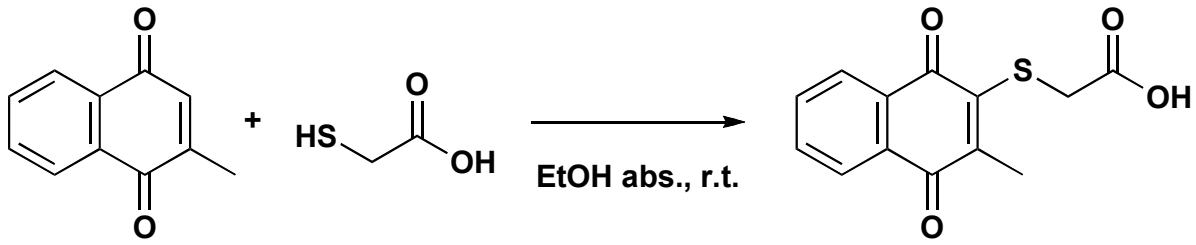

[172.18] [92.12] [262.28]

Synthesis

Thioglycolic acid (126 µL, 1.39 mmol, 1.2 eq) was added to a suspension of menadione (200 mg, 1.16 mmol, 1 eq) in dry ethanol (10 mL) (orange → brown). The reaction mixture was stirred for 24 hours at room temperature under an argon atmosphere and afterwards concentrated *in vacuo*. The residue was dissolved in ethyl acetate and extracted with sodium bicarbonate (saturated solution). The bicarbonate extracts were acidified with concentrated hydrochloric acid and extracted with dichloromethane. The solvent was evaporated under reduced pressure yielding the desired product.

Yield: 173 mg (57%), yellow/orange solid

Elemental analysis for $C_{13}H_{10}O_4S$

	C [%]	H [%]	O [%]	S [%]
calculated	59.53	3.84	24.40	12.23
found	59.96	4.15	-	11.92
Δ	-0.43	-0.31	-	0.31

NMR-spectroscopy

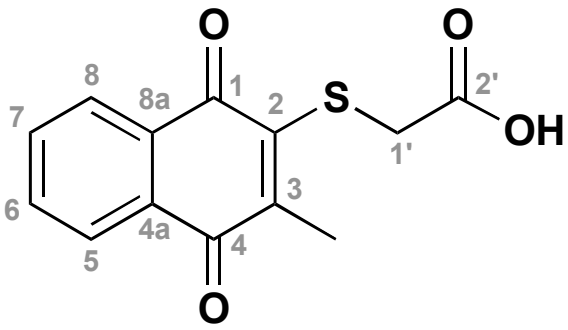

^{1}H NMR (500.10 MHz, DMSO-d_6) δ: 12.72 (s, 1H, COOH), 8.03 – 7.96 (m, 2H, H-6, H-7), 7.87 – 7.81 (m, 2H, H-5, H-8), 3.98 (s, 2H, H-1'), 2.26 (s, 3H, CH_3).

3.2.1.3 2-Chloro-3-(2-hydroxyethylthio)naphthalene-1,4-dione (4)

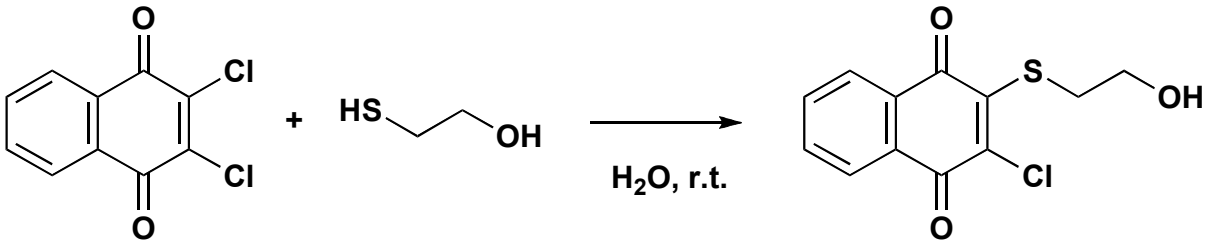

[227.04] [78.13] [268.72]

Synthesis

2,3-Dichloro-1,4-naphthoquinone (100 mg, 0.44 mmol, 1 eq) was suspended in water (25 mL) and mercaptoethanol (34 µL, 0.484 mmol, 1.1 eq) was added. The reaction mixture was stirred for 16 hours at room temperature. The product was filtered, washed with water and dried.

Yield 105 mg (90%), orange powder

Elemental analysis for $C_{12}H_9ClO_3S$

	C [%]	H [%]	O [%]	S [%]
calculated	53.64	3.38	17.86	11.93
found	53.91	3.58	17.89	13.96
Δ	-0.27	-0.20	-0.03	-2.03

NMR-spectroscopy

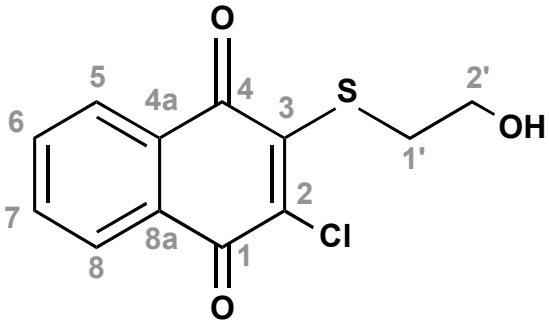

^{1}H NMR (500.10 MHz, DMSO-d_6) δ: 8.13 – 8.07 (m, 1H, H-6/H-7), 7.97 – 7.94 (m, 1H, H-7/H-6), 7.93 – 7.90 (m, 1H, H-5/H-8), 7.84 – 7.78 (m, 1H, H-8/H-5), 4.90 (t, ^{3}J(H,H) = 5 Hz, 1H, OH), 3.61 (dt, ^{3}J(H,H) = 6 Hz, ^{3}J(H,H) = 6 Hz, 2H, H-2'), 3.29 (t, ^{3}J(H,H) = 6 Hz, 2H, H-1').

3.2.1.4 2-(3-Chloro-1,4-dioxo-1,4-dihydronaphthalen-2-ylthio)acetic acid (5)

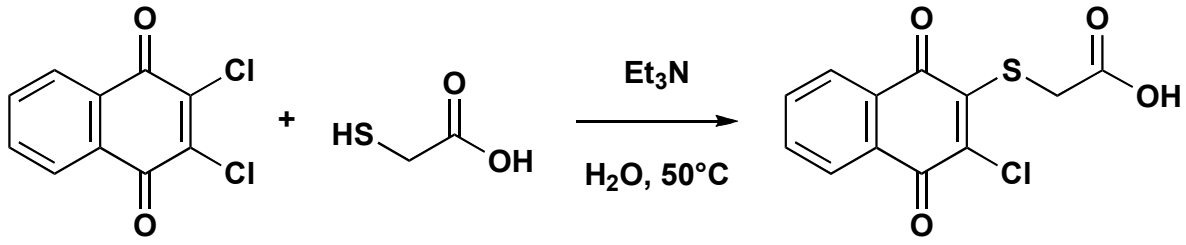

[227.04] [92.12] [282.70]

Synthesis

Triethylamine (245 µL, 1.76 mmol, 4.0 eq) were added to a suspension of 2,3-dichloro-1,4-naphthoquinone (100 mg, 0.44 mmol, 1 eq) in water (3 mL) (→green). Thioglycolic acid (44 µL, 0.48 mmol, 1.1 eq) was added (→dark red) and the reaction mixture was stirred for 3 hours at 50 °C. The solvent was evaporated under reduced pressure, the residue was dissolved in dichloromethane, extracted three times with sodium bicarbonate (saturated solution), acidified with concentrated hydrochloric acid, extracted subsequently three times with dichloromethane and concentrated under reduced pressure yielding the desired product.

Yield 108.6 mg (87%), orange solid

(ESI$^+$) *m/z* 282.0

NMR-spectroscopy

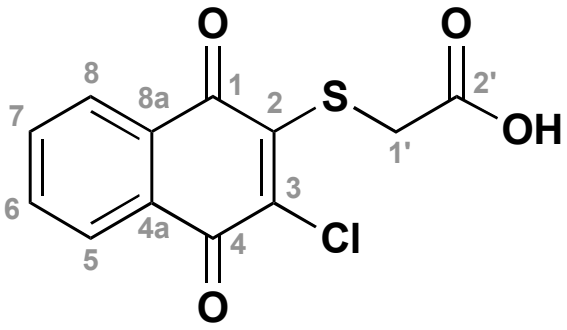

^{1}H NMR (500.10 MHz, DMSO-d_6) δ: 8.02 – 7.94 (m, 2H, H-6, H-7), 7.85 – 7.77 (m, 2H, H-5, H-8), 3.79 (s, 2H, H-1').

3.2.3 GENERAL COMPLEXATION OF O,S-CHELATES

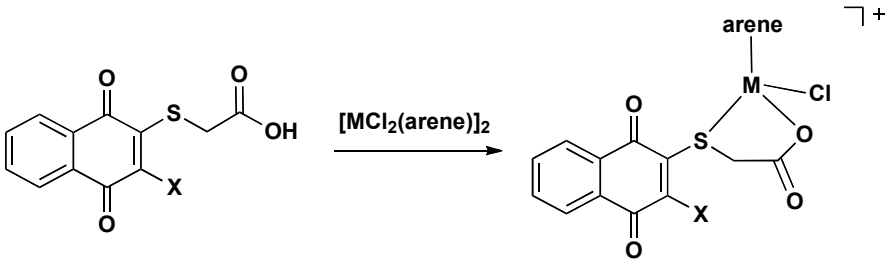

Figure 31: General procedure for the complexation of O,S-chelates; X = CH_3 (3), Cl (5); $[MCl_2(arene)]_2$ (a M = Ru^{II}, b M = Os^{II}, arene = η^6-*p*-cymene).

A solution of the corresponding arene dimer precursor in dry dichloromethane was added to a solution of ligand **3** or **5** under alkaline conditions (NaOMe, Et_3N, NaOH, NMM) in (dry)MeOH, (dry)EtOH, (dry)DCM, or toluol (Figure 31). The reaction mixture was whether stirred for 1-24 h at room temperature or refluxed for 1-24 h and under argon atmosphere. Approaches with microwave synthesis were performed using different temperatures and reaction times. The solvent was evaporated *in vacuo*, the residue was dissolved in dichloromethane and filtered. The filtrate was concentrated under reduced pressure to a volume of about 3 mL, and *n*-hexane was added to precipitate the product.

3.2.4 HPLC SEPARATION STUDIES

3.2.4.1 Analytical HPLC analysis

The experimental conditions for the chromatographic system were as follows: stationary phase: silica-based C18 gel (XBridge C18 5 µm, 4.6 mm x 150 mm); mobile phase: 15 mM HCOOH, MeOH; flow rate: 1.00 mL/min, injection volume: 25 µL; column temperature: 25 °C; UV/Vis detection: 225 nm, 250 nm, 275 nm and 300 nm.

3.2.4.2 Preparative HPLC

For product purification, preparative reversed phase HPLC was performed on a silica based C18 Waters Xbridge Column on an Agilent 1200 Series system, which was controlled by Chemstation software. The column was temperature-controlled at 20 °C and the flow rate was constant at 17 mL/min.

3.3 LAPACHOL

3.3.1 SYNTHESIS OF DIMERIC METAL PRECURSORS

3.3.1.1 Bis[(η^6-*p*-cymene)dichloridoruthenium(II)]

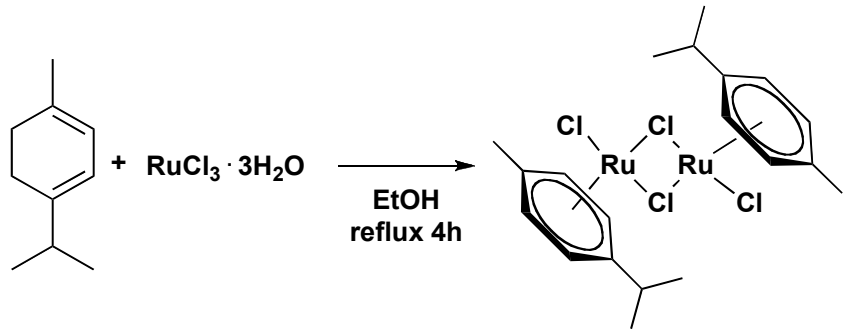

[134.21] [261.47] [612.39]

Synthesis

α-Terpinene (12.5 mL, 77 mmol) was added to a solution of the $RuCl_3 \cdot 3H_2O$ (2.0 g, 7.6 mmol) in dry ethanol (75 mL) and the reaction mixture was refluxed for 4 h. After cooling the mixture to room temperature, the volume was reduced to 30 mL and diethyl ether (40 mL) was added. The obtained red solid was filtered off, washed with diethyl ether (3 x 10 mL) and dried *in vacuo*.

Yield 8.57 g (92%), red powder

Melting point >182 °C (decomposition)

NMR-spectroscopy

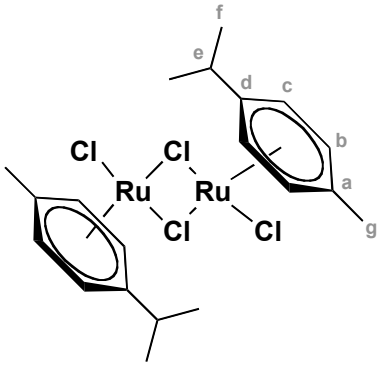

^{1}H-NMR (500.10 MHz, $CDCl_3$) δ: 5.47 (d, ^{3}J(H,H) = 6 Hz, 2H, H-c), 5.34 (d, ^{3}J(H,H) = 6 Hz, 2H, H-b), 2.88 – 2.96 (m, 1H, H-e), 2.16 (s, 3H, H-g), 1.28 (d, ^{3}J(H,H) = 7 Hz, 6H, H-f).

^{13}C-NMR (125.75 MHz, $CDCl_3$) δ: 101.2 (C_d), 96.7 (C_a), 81.3 (Cc), 80.5 (C_b), 30.6 (C_e), 22.2 (C_f), 18.9 (C_g).

3.3.1.2 Bis[(η^6-*p*-cymene)dichloridoosmium(II)]

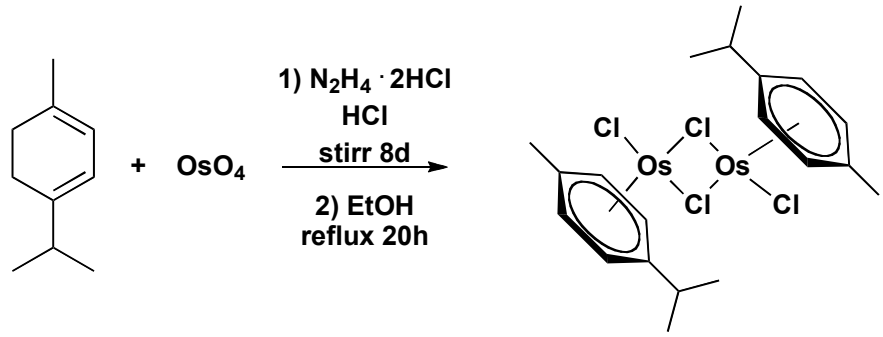

[134.21] [254.23] [790.71]

Synthesis

Hydrochloric acid 37% (90 mL) was added to hydrazine dihydrochloride (840 mg, 8 mmol) in a 100 mL round-bottom flask, equipped with a $CaCl_2$ drying tube. Afterwards, osmiumtetroxide (2.00 g, 7.9 mmol) was added and the mixture was stirred for 8 days under light exposure.

The red solution was filtered and the solvent was evaporated. The remaining oil was dissolved in dry EtOH (30 mL), transferred to a 100 mL round-bottom flask and concentrated to dryness. The residue was again dissolved in dry EtOH (50 mL) and the evaporated to dryness. The obtained red oil was flushed 3 times with argon and redissolved in dry EtOH (50 mL). α-Terpinene was added to the red solution and refluxed for 20 hours under light exclusion and argon atmosphere.

Afterwards, the solution was allowed to cool to room temperature and stored at -20 °C for 2 weeks. The formed orange solid was filtered off, washed with acetone and dried *in vacuo*.

Yield 4.21 g (34%), red powder

NMR-spectroscopy

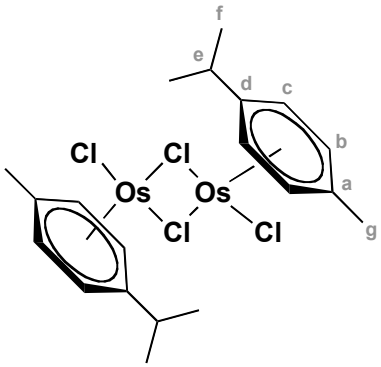

^{1}H-NMR (500.10 MHz, $CDCl_3$) δ: 6.18 (d, ^{3}J(,HH) = 6 Hz), 2H, H-c), 6.02 (d, ^{3}J(,HH) = 6 Hz), 2H, H-b), 2.78 (hept, ^{3}J(H,H) = 7 Hz, 1H, H-e), 2.20 (s, 3H, H-g), 1.29 (d, ^{3}J(,HH) = 7 Hz, 6H, H-f).

3.3.1.3 Bis[(η^5-pentamethylcyclopentadienyl)dichloridorhodium(III)]

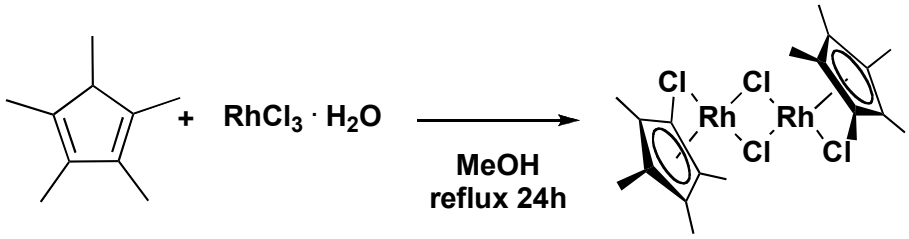

[136.24] [209.26] [618.09]

Synthesis

$RhCl_3 \cdot H_2O$ (1.7 g, 6.5 mmol, 0.45 eq) was suspended in methanol (50 mL) and pentamethylcyclopentadiene (1.1 mL, 7.1 mmol, 1.1 eq) was added. The mixture was refluxed for 24 hours. The reaction mixture was cooled to r.t., the formed red solid was filtered and used without further purification.

Yield 415.8 mg (75%), red powder

Melting point 152–154 °C

NMR-spectroscopy

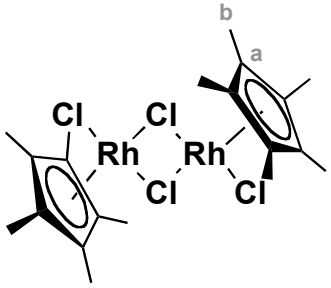

^{1}H-NMR (500.10 MHz, $CDCl_3$) δ: 1.62 (s, 30H, H-b).

^{13}C-NMR (125.75 MHz, $CDCl_3$) δ: 94.3 (10C, C_a), 9.5 (10C, C_b).

3.3.2 SYNTHESIS OF LAPACHOL COMPLEXES

3.3.2.1 General procedure for the synthesis of lapachol complexes

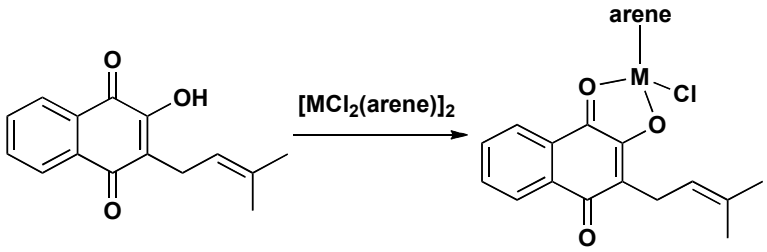

L 1a-c

Figure 32: Synthesis of the organometallic lapachol (L) complexes 1a-c: (i) NaOMe, $[MCl_2(arene)]_2$ (a M = Ru^{II}, b M = Os^{II}, arene = η^6-*p*-cymene; c M = Rh^{III}; arene = η^5-pentamethylcyclopentadiene).

A solution of the corresponding arene dimer complex in dry dichloromethane was added to a solution of lapachol and sodium methoxide in dry methanol (Figure 32). The reaction mixture was stirred for 4.5 or 24 h at room temperature and under argon atmosphere. The solvent was evaporated *in vacuo*, the residue was dissolved in dichloromethane and filtered. The filtrate was concentrated under reduced pressure to a volume of about 3 mL, and *n*-hexane was added to give the pure product (needles, crystals) in good to excellent yields (75-96%).

3.3.2.2 Chlorido[(3-(3-methylbut-2-enyl)-2-oxo-κ*O*)-1,4-naphthoquinonato-κ*O*](η^6-*p*-cymene)ruthenium(II) (1a)

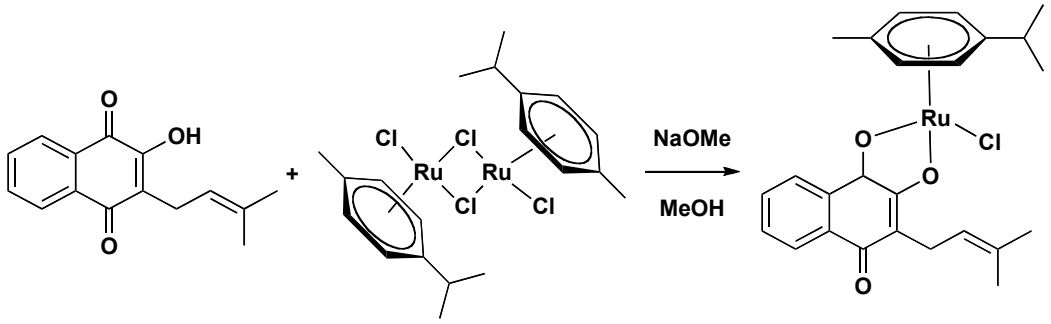

[242.27] [612.39] [512.00]

Synthesis

The reaction was performed according to the general procedure, using lapachol (88 mg, 0.36 mmol, 1 eq), NaOMe (22 mg, 0.40 mmol, 1.1 eq) and bis[(η^6-*p*-cymene)dichloridoruthenium(II)] (100 mg, 0.16 mmol, 0.9 eq) with a reaction time of 4.5 hours.

Yield 171.2 mg (92%), dark blue needles

Melting point 148–150 °C

Solubility 290 µM in 1% DMSO/PBS

(ESI$^+$) *m/z* 477.11 $[M - Cl]^+$

Elemental analysis for $C_{25}H_{27}ClO_3Ru \cdot 0.5H_2O$

	C [%]	H [%]
calculated	57.63	5.42
found	57.57	5.11
Δ	0.06	0.31

NMR-spectroscopy

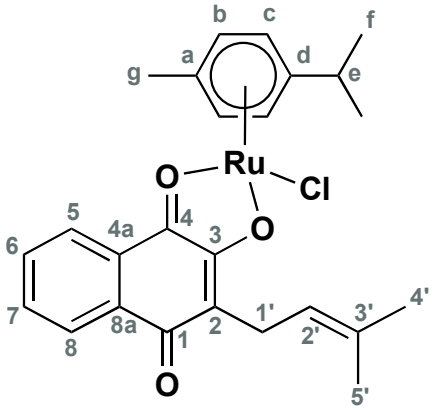

^{1}H NMR (500.10 MHz, $CDCl_3$) δ: 8.00 (d, ^3J(H,H) = 8 Hz, 1H, H-5), 7.96 (d, ^3J(H,H) = 8 Hz, 1H, H-8), 7.68 (ddd, ^3J(H,H) = 8 Hz, ^3J(H,H) = 8 Hz, ^4J(H,H) = 2 Hz, 1H, H-7), 7.51 (ddd, ^3J(H,H) = 8 Hz, ^3J(H,H) = 8 Hz, ^4J(H,H) = 2 Hz, 1H, H-6), 5.80–5.73 (m, 2H, H-c), 5.54–5.46 (m, 2H, H-b), 5.31–5.26 (m, 1H, H-2'), 3.43–3.25 (m, 2H, H-1'), 3.03–2.96 (m, 1H, H-e), 2.40 (s, 3H, H-g), 1.82 (s, 3H, H-4'), 1.68 (s, 3H, H-5'), 1.42 (d, ^3J(H,H) = 8 Hz, 6H, H-f).

$^{13}C\{^1H\}$ NMR (125.75 MHz, d_4-CH_3OH) δ: 196.2 (C_4), 182.7 (C_1), 169.1 (C_3), 136.1 (C_7), 132.6 (C_{8a}), 131.7 (C_6), 131.2 ($C_{3'}$), 127.9 (C_{4a}), 125.8 (C_5), 125.7 (C_8), 125.3 (C_2), 121.6 ($C_{2'}$), 100.5 (C_d), 96.9 (C_a), 81.03 (C_c), 79.0 (C_b), 31.1 (C_e), 24.3 ($C_{5'}$), 21.6 ($C_{1'}$), 21.0 (C_f), 17.1 (C_g), 16.6 ($C_{4'}$).

3.3.2.3 Chlorido[(3-(3-methylbut-2-enyl)-2-oxo-κ*O*)-1,4-naphthoquinonato-κ*O*] (η^6-*p*-cymene)osmium(II) (1b)

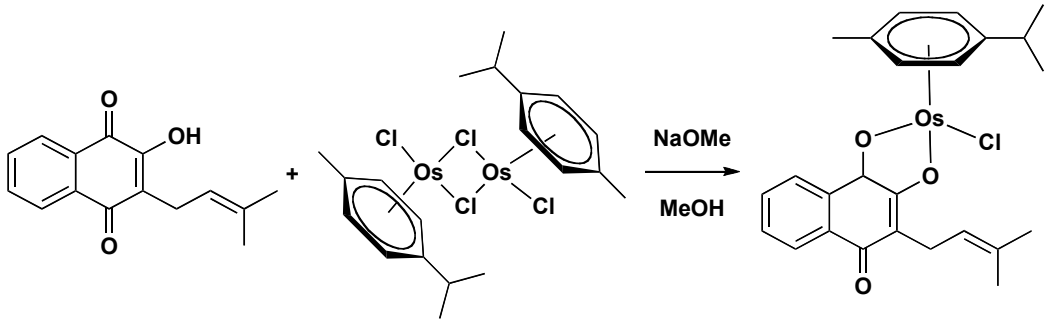

[242.27] [790.71] [601.16]

Synthesis

The reaction was performed according to the general procedure, using lapachol (65 mg, 0.27 mmol, 1 eq), NaOMe (16 mg, 0.29 mmol, 1.1 eq) and bis[(η^6-*p*-cymene)dichloridoruthenium(II)] (100 mg, 0.13 mmol, 0.95 eq) with a reaction time of 4.5 hours.

Yield 113.3 mg (75%), dark blue crystals

Melting point 148–150 °C

Solubility 170 µM in 1% DMSO/PBS

(ESI$^+$) *m/z* 567.16 $[M\text{-}Cl]^+$

Elemental analysis for $C_{25}H_{27}ClO_3Os$

	C [%]	H [%]
calculated	49.95	4.53
found	49.94	4.22
Δ	0.01	0.31

NMR-spectroscopy

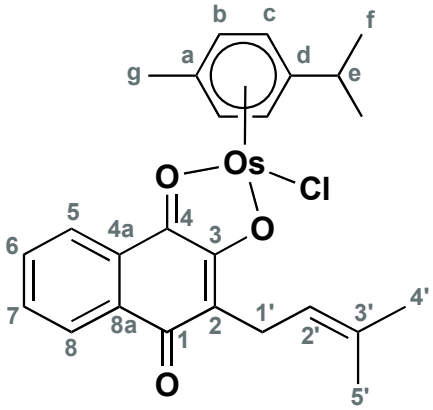

^{1}H NMR (500.10 MHz, $CDCl_3$) δ: 8.02 (d, ^3J(H,H) = 8 Hz, 1H, H-5), 8.00 (d, ^3J(H,H) = 8 Hz, 1H, H-8), 7.72 (ddd, ^3J(H,H) = 8 Hz, ^3J(H,H) = 8 Hz, ^4J(H,H) = 2 Hz, 1H, H-7), 7.54 (ddd, ^3J(H,H) = 8 Hz, ^3J(H,H) = 8 Hz, ^4J(H,H) = 2 Hz, 1H, H-6), 6.25–6.19 (m, 2H, H-c), 5.96–5.89 (m, 2H, H-b), 5.31–5.25 (m, 1H, H-2'), 3.40–3.29 (m, 2H, H-1'), 2.89–2.80 (m, 1H, H-e), 2.43 (s, 3H, H-g), 1.80 (s, 3H, H-4'), 1.67 (s, 3H, H-5'), 1.39 (d, ^3J(H,H) = 8 Hz, 6H, H-f).

$^{13}C\{^1H\}$ NMR (125.75 MHz, $CDCl_3$) δ: 198.6 (C_4), 182.8 (C_1), 169.8 (C_3), 136.3 (C_7), 132.9 (C_{8a}), 132.1 ($C_{3'}$), 131.3 (C_6), 127.9 (C_{4a}), 127.0 (C_2), 126.7 (C_5), 126.5 (C_8), 121.7 ($C_{2'}$), 90.8 (C_d), 88.0 (C_a), 72.4 (C_c), 69.1 (C_b), 32.1 (C_e), 25.8 ($C_{5'}$), 22.8 ($C_{1'}$), 22.6 (C_f), 19.1 (C_g), 18.1 ($C_{4'}$).

3.3.2.4 Chlorido[(3-(3-methylbut-2-enyl)-2-oxo-κ*O*)-1,4-naphthoquinonato κ*O*](η^5-pentamethylcyclopentadienyl)rhodium(III) (1c)

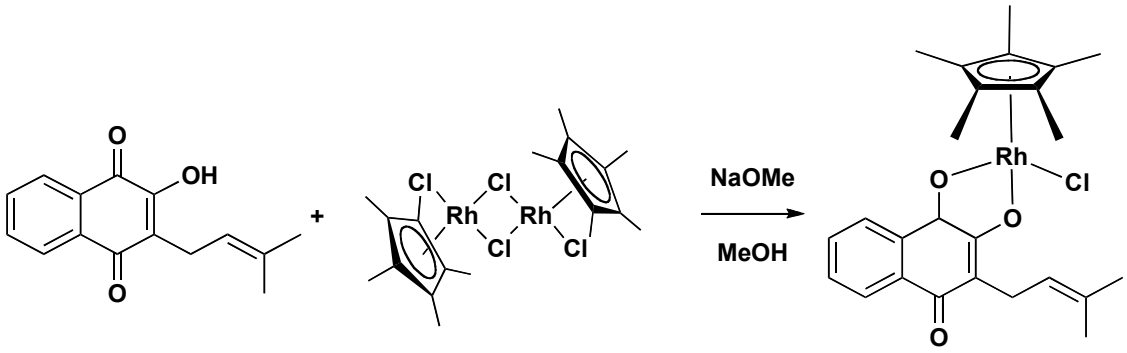

[242.27] [618.09] [514.85]

Synthesis

The reaction was performed according to the general procedure, using lapachol (83 mg, 0.34 mmol, 1.00 eq), NaOMe (20 mg, 0.38 mmol, 1.10 eq) and bis[(η^6-*p*-cymene)dichloridoruthenium(II)] (100 mg, 0.16 mmol, 0.95 eq) with a reaction time of 24 hours.

Yield 160.4 mg (96%), dark violet needles

Melting point 144–146 °C

Solubility 190 µM in 1% DMSO/PBS

(ESI$^+$) *m/z* 479.10 $[M\text{-}Cl]^+$

Elemental analysis for $C_{25}H_{28}ClO_3Rh$

	C [%]	H [%]
calculated	58.32	5.48
found	58.59	5.62
Δ	-0.27	-0.14

NMR-spectroscopy

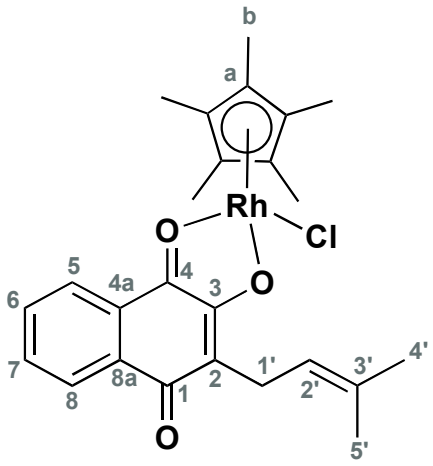

^{1}H NMR (500.10 MHz, $CDCl_3$) δ: 7.99 (d, ^3J(H,H) = 7 Hz, 1H, H-5), 7.98 (d, ^3J(H,H) = 7 Hz, 1H, H-8), 7.69–7.64 (m, 1H, H-7), 7.51–7.46 (m, 1H, H-6), 5.36–5.30 (m, 1H, H-2'), 3.42–3.24 (m, 2H, H-1'), 1.82 (s, 3H, H-4'), 1.67 (s, 3H, H-5').

^{13}C{^{1}H} NMR (125.75 MHz, CDCl3) δ: 194.8 (C_4), 182.9 (C_1), 168.5 (C_3), 135.7 (C_7), 133.5 (C_{8a}), 131.3 ($C_{3'}$), 131.0 (C_6), 129.1 (C_{4a}), 126.3 (C_5), 126.2 (C_8), 125.6 (C_2), 122.6 ($C_{2'}$), 92.9 (C_a), 25.8 ($C_{5'}$), 22.8 ($C_{1'}$), 18.2 ($C_{4'}$), 9.1 (C_b).

3.3.3 UV/VIS AND AQUEOUS SOLUTION BEHAVIOR

The test substance was dissolved in DMSO and subsequently diluted with PBS to a final concentration of 50 µM in 1% DMSO/PBS solution. UV/Vis spectra were instantly recorded with a Perkin Elmer Lambda 650 spectrophotometer equipped with a six cell changer and a Peltier element for temperature control or an Agilent 8453 spectrophotometer. Spectra were repeated for at least 10 times the first 10 minutes and then after 24, 48 and 72 hours.

3.3.4 ESI-MS STABILITY AND BIOMOLECULE INTERACTION STUDIES

3.3.4.1 Materials

Dimethylsulfoxide (DMSO) was obtained from Acros; formic acid (98%) and L-cysteine (Cys) from Fluka; glycine (Gly) and L-histidine (His) from Merck; ubiquitin (ub, bovine erythrocytes) and 9-ethylguanine (EtG) from Sigma; L-methionine (Met) from Sigma-Aldrich and tetramethylammonium acetate from TCI Europe. MilliQ water (18.2 MΩ; Millipore Advantage A10, 185 UV Ultrapure Water System, Molsheim, France) and methanol (HPLC grade, Fisher) were used for ESI-MS studies.

3.3.4.2 Instrumentation

Electrospray ionization mass spectra were recorded on a Bruker AmaZon SL ion trap (ESI-IT) and a UHR MaXis time-of-flight (ESI-TOF) mass spectrometer (Bruker Daltonics GmbH, Bremen, Germany). Experimental data was acquired and processed using Compass 1.3 and Data Analyis 4.0 (Bruker Daltonics GmbH, Bremen, Germany). In-source collision-induced dissociation (ISCID) was performed on the ESI-TOF-MS using collision energies of 90 eV. Deconvolution was obtained by automatic data point spacing and 30000 instrument resolving power. The accuracy of the ESI-TOF measurement was calculated in Δppm, while the measurements on the ESI-IT include a standard deviation of m/z ± 0.05. ESI-IT-MS spectra were recorded in the positive ion mode using the following parameters: capillary -4.5 kV, nebulizer 8 psi, dry gas 6 L/min, dry temperature 180 °C, accumulation time 0.1 ms and trap drive 57%. Similar parameters were used for recording ESI-TOF mass spectra: capillary -4.5 kV, nebulizer 5.8 psi, dry gas 6 L/min and dry temperature 180 °C. Finally, samples for ESI-MS were introduced by direct-infusion into the mass spectrometer at a flow rate of 4 µL/min.

3.3.4.3 Sample preparation

Stock solutions of **1a–c** (50–100 µM) were prepared in water using 1% DMSO. Additionally, stock solutions were prepared of ub (200 µM) and a mixture of EtG : Cys : Gly : His : Met (1 : 1 : 1 : 1 : 1) containing 400 µM of each compound in water. The three compounds were independently incubated with ub at a 2 : 1 metal-to-protein ratio and with the amino acid/model nucleobase mixture at a 1 : 1 molar ratio giving final metal concentrations of 25–50 µM. All mixtures were incubated in the absence of light. Experiments in buffered solution contained tetramethylammonium acetate buffer (2.5 mM, pH ≈ 8.5). Mass spectra of the incubation solutions were recorded directly after mixing and after 1, 3, 6 and 24 h. Small molecule samples were diluted with H_2O : MeOH (1 : 1), while the protein samples were diluted with H_2O : MeOH : formic acid (50 : 50 : 0.2) to a final metal concentration of 1 – 5 µM prior to infusion into the mass spectrometer. The protein samples were therefore analyzed under denaturing conditions leading to the rupture of the protein tertiary structure.

3.3.5 CYTOTOXICITY IN CANCER CELL LINES

3.3.5.1 Cell lines and culture conditions

CH1 cells (adenocarcinoma of the ovary, human) were provided by Lloyd R. Kelland (CRC Centre for Cancer Therapeutics, Institute of Cancer Research, Sutton, U.K). SW480 (adenocarcinoma of the colon, human) and A549 (non-small cell lung cancer, human) cells were purchased from ATCC. All cell culture reagents were purchased from Sigma-Aldrich. Cells were grown in 75 cm^2 culture flasks (Starlab) as adherent monolayer cultures in complete culture medium, *i.e.* Eagle's minimal essential medium (MEM) supplemented with 10% heat-inactivated fetal calf serum, 1 mM sodium pyruvate, 4 mM L-glutamine, and 1% non-essential amino acids (from 100× ready-to-use stock) without antibiotics. Cultures were maintained at 37 °C in a humidified atmosphere containing 95% air and 5% CO_2.

3.3.5.2 MTT assay conditions

Cytotoxicity was determined by the colorimetric MTT (3-(4,5-dimethyl-2-thiazolyl)-2,5-diphenyl-2*H*-tetrazolium bromide, purchased from Fluka) microculture assay. For this purpose, cells were harvested from culture flasks by trypsinization and seeded in 100 µL/well aliquots of complete culture medium into 96-well microculture plates (Starlab). Cell densities of 1×10^3 cells/well (CH1), 2×10^3 cells/well (SW480) and 3×10^3 cells/well (A549) were chosen in order to ensure exponential growth of untreated controls throughout the experiment. For 24 h, cells were allowed to settle and resume exponential growth. The test compounds were dissolved in DMSO, serially diluted in complete culture medium (such that the DMSO content in actual test solutions did not exceed 0.5%) and added in 100 µL/well aliquots for an exposure time of 96 hours. At the end of exposure, the medium was replaced with 100 µL/well of a 7:1 mixture of RPMI1640 culture medium (supplemented with 10% heat-inactivated fetal calf serum) and MTT solution in phosphate-buffered saline (5 mg/mL). After incubation for 4 h, the supernatants were removed, and the formazan crystals formed by viable cells were dissolved in 150 µL DMSO per well. Optical densities at 550 nm were measured with a microplate reader (BioTek ELx808), using a reference wavelength of 690 nm to correct for unspecific absorption. The quantity of viable cells was expressed in terms of T/C values by comparison to untreated control microcultures, and 50% inhibitory concentrations (IC_{50}) were calculated from concentration-effect curves by

interpolation. Evaluation is based on means from at least three independent experiments, each comprising three replicates per concentration level.

3.3.5.3 ROS Assay

For the fluorimetric analysis of reactive oxygen species (ROS) non-adherent HL60 cells (promyelocytic leukemia, human) were stained for 30 min at 37 °C and 5% CO_2 with 0.1 µM DCFH-DA (2',7'-dichlorofluorescein diacetate) in Hank's Salt Solution supplemented with 1% bovine serum. $5 \times 10^4 – 8 \times 10^4$ cells/well were transferred to 96-well plates and treated directly with the test substances at different concentrations for 30 min at 37 °C, 5% CO_2. 500 µM freshly prepared H_2O_2 solution was used as a positive control and added 10 min before measurement. The generated ROS activity within the cells was measured on a Guava easyCyte 8HT device (Millipore). The resulting histograms of green fluorescence were quantified by FlowJo software (Tree Star). Green fluorescence intensity is defined as the ratio between the drug-treated sample and the untreated control.

3.3.5.4 Cell Cycle Analysis

HFS buffer (hypotonic fluorochrome solution) was prepared using 0.1% (V/V) Triton X-100, 0.1% (W/V) sodium citrate, in PBS. CH1 cells (1×10^5) in MEM medium were seeded into 12-well microculture plates (Starlab) and allowed to recover for 24 h. Cells were then treated with different concentrations of the test compounds for 24 h at 37 °C, 5% CO_2. Controls (negative: Eagle's minimal essential medium, positive: 0.01 and 0.05 µM gemcitabine) and drug-treated cells were collected, washed with PBS, and stained in 600 µL propidium iodide/HFS solution (50 µg/mL) for 24 h in the dark at 4 °C. Fluorescence was measured by flow cytometry by using a Guava easyCyte 8HT instrument (Millipore). The resulting histograms of red fluorescence were quantified by FlowJo software (Tree Star).

4 CONCLUSION AND OUTLOOK

In summary, several naphthoquinones, modified *via* reaction with different thiols, were synthesized in good to excellent yields according to reproducible and sustainable procedures. These potential *O,S*-chelates have been reported in literature to exhibit promising anticancer activity. All compounds were characterized *via* ^{1}H – NMR and elemental analysis. It was possible in some cases to coordinate the prepared *O,S*-chelating ligands to a metal center, however, purification of the obtained mixtures failed. Further investigations have to be performed to identify the obtained product species and separate the (different) species.

Organometallic lapachol complexes were prepared in high yields, which are activated by fast hydrolysis to the corresponding aqua species in aqueous solution. They are able to interact with biomolecules and show antiproliferative activity in the low µM range in human tumor cell lines. The first investigations of the underlying mechanisms showed an enhanced anticancer activity, especially in case of **1a**, based on ROS-induced cell cycle arrest. Further investigations will elucidate the mode of action in more detail. Overall, the ruthenium complex **1a** induced generation of reactive oxygen species to a higher degree compared to lapachol and its rhodium and osmium analogues, and shows further on a higher cytotoxicity on all investigated cancer cell lines, demonstrating a synergistic effect of the ruthenium center and the bioactive ligand. Due to the high and promising cytotoxicity of the ruthenium lapachol complex and the high stability of the rhodium compound in aqueous solution, both organometallic complexes were submitted for further *in vivo* experiments.

In summary it can be mentioned, that the developed work concerns synthetic, but also analytical and cell biological studies and hence conveys an interdisciplinary overview over organometallic synthetic chemistry associated with current cancer research, the use of different analytical methods and the work in the cell culture.

CURRICULUM VITAE

Evelyn Balsano, B.Sc.

Moritzinger Feldweg 13 K

39100 Bolzano, Italy

0043 0650 3524040

evelyn.balsano@univie.ac.at

PERSONAL INFORMATION

Nationality	Italian
Date of birth	10 August 1985
Place of birth	Bolzano, Italy

LANGUAGE SKILLS

Grown up bilingual: German and Italian;
English (fluent), French (fluent), Spanish (beginner)

EDUCATION

Currently	Master thesis in Bioinorganic Chemistry at the University of Vienna – Institute of Inorganic Chemistry (O. Univ.-Prof. Dr. Dr. Bernhard K. Keppler and DI Dr. Wolfgang Kandioller)
Since 2010	Master program Chemistry University of Vienna
2010	Bachelor of Science University of Vienna Bachelor thesis at the University of Vienna – Institute of Analytical Chemistry (Ao. Univ.-Prof. Mag. Dr. Peter Lieberzeit) Spectroscopic and microscopic studies of thiol immobilization on gold surfaces
2006 – 2010	Bachelor program Chemistry University of Vienna
1999 – 2004	Humanistisches Gymnasium neusprachlicher Fachrichtung in Bozen (German, Italian, English, French, Latin)
1996 – 1999	Mittelschule Aufschnaiter Bolzano (Italy)
1991 – 1996	Grundschule Karl Wolff Bolzano (Italy)

STAY ABROAD

Winter semester 2011-2012	Chemistry study at the University of Ottawa in Canada

SCIENTIFIC INTERESTS

Organic and Organometallic Synthetic Chemistry
Cell biology
Biochemistry
Ecotoxicology
Environmental Chemistry
Environmental Analytical Chemistry

RESEARCH AREAS AND RESEARCH TECHNIQUES

2012	University of Vienna Supervisor O. Univ.-Prof. Dr. Dr. Bernhard K. Keppler Master student Synthesis, Characterization und Analysis of organic and organometallic compounds Working in inert atmosphere Microwave synthetic chemistry Analytics: UV/Vis, HPLC, Biological Tests: MTT, FACS (Cell Cycle Analysis, ROS assay)
2010	University of Vienna Supervisor Ao. Univ.-Prof. Mag. Dr. Peter Lieberzeit Bachelor student Preparation of gold surfaces, investigation of SAM with STM, QCM in gaseous phase, IR-spectroscopy

TEACHING EXPERIENCE

Winter semester 2011 – 2012	Tutor at the University of Vienna for the advanced organic synthetic laboratory
Summer semester 2011	Tutor at the University of Vienna for the advanced organic synthetic laboratory
February 2011	Teacher (Grundschule Vilpian)
Summer semester 2010	Tutor at the University of Vienna for nutritionists and biologists
School year 2004 – 2005	Teacher at different elementary and secondary schools in South Tirol (Italy)

FURTHER WORK EXPERIENCE

Summer 2008	Animation Camping „Les Sérignan Plage Nature“ in France
Summer 2007	Receptionist Camping „Les Sérignan Plage Nature“ in France
Summer 2006	Receptionist Camping „Les Sérignan Plage Nature“ in France
Summer 2003	Waitress in Oberbozen
2001 – 2002	Animation and private nanny (Parkhotel Holzner in Oberbozen)

VOLUNTARY WORK

2003	Jungscharleiterin (I organized in collaboration with colleagues afternoons for children and youths: Games, Sport, Music, Singing, Dance, Theaters…)

SCHOLARSHIP

2012	Leistungsstipendium im Ausland, Autonome Provinz Bozen Südtirol
2010	Joint Study Stipendium Non- EU student exchange program University of Vienna

COMPUTER LITERACY

Microsoft Office	Word, Excel, Powerpoint
Adobe programs	Illustrator, InDesign, Photoshop
Chemical softwares	Chemdraw, MestRenova, FlowJo

HOBBIES

Languages, Travelling, Communication with people from all over the world, Dance, Hiking, Art, Cooking.